RADIATION STUDIES IN SPACE WITH NUCLEAR EMULSION DETECTORS

HERMAN YAGODA
Air Force Cambridge Research Laboratories, Geophysics Research Directorate, Bedford, Massachusetts, U.S.A.

(Received August 15, 1962)

1. Introduction

The photographic emulsion is a well known device for the study of ionizing radiations having a rather venerable antiquity. It was the tool which led BECQUEREL in 1896 to the discovery of radioactivity and has since played an important role in the development of nuclear physics. Among the important discoveries made with this quasi-solid state detector was the production of secondary stars as a result of the interaction of primary cosmic radiation with the nuclei of atmospheric constituents (BLAU, 1937). The elucidation of the properties of the π-meson (LATTES *et al.*, 1947) showing it to be the long sought for bonding particle which stabilizes complex nuclei from disintegration by their internal electrostatic repulsive forces as first predicted by YUKAWA (1935), stimulated the further use of emulsions by physicists throughout the world. Among their findings, first by exposure to cosmic radiation on mountain tops and subsequently in experiments utilizing high energy accelerators, was the discovery of the existence of a host of fundamental particles which the perplexed theoreticians dubbed the strange particles because while created in very fast interactions they decayed comparatively slowly. One category of these, such as the tau, theta and kappa mesons, left tracks in the emulsions whose grain density and scattering parameters indicated a mass intermediate between that of the π-meson and the proton, vis 966 m_e. A second category of unstable particles was proven to be produced in high energy interactions of greater than protonic mass such as the Λ°-particle which decayed into a proton and a negatively charged π-meson, and the cascade particle of 2580 m_e. Another group of investigators flying small blocks of emulsions in Skyhook balloons near the top of the atmosphere observed the tracks produced by multiple-charged particles of Z $\geqq$ 2, the heavy primaries.

The utilization of the emulsion as an ionizing particle detector reached a slow maximum with the discovery of the anti-proton. Subsequently, its use in conjunction with accelerator studies gradually declined with the advent of the liquid bubble chamber. This non-integrating charged particle detector has the advantage in simplifying the interpretation of results, particularly when the composition of the target is mono-atomic as is the case when liquid hydrogen serves as the medium. The need for massive refrigerating equipment has kept this new competing detector for delineating the spatial orientation of charged particles essentially land based. The nuclear emulsion is still employed extensively in the study of the primary cosmic radiation at points high in the atmosphere and cooperative groups endeavouring to elucidate the rare ultra-energetic particles with kinetic energies in excess of 10^{12} ev have exposed large blocks of emulsions weighing up to 800 pounds by means of polyethyelene balloons. Smaller payloads can be carried up to 42 km by means of 10 million cubic foot balloons where the vertical air mass is only 2.4 g. cm^{-2}.

At the end of World War II a group of captured German V-2 rockets were brought to the White Sands Proving Grounds in New Mexico (geomagnetic latitude 41° N) and the war-heads were reconstructed as a housing for upper air research. The experiments were largely designed so that the observations could be transmitted to ground stations by telemetry. The instruments were considered expendable as the rocket was buried deep underground on impact after falling from apogee's of approximately 100 miles. Certain kinds of information could not be telemetered, such as photographs of the sun's spectrum above the atmosphere, and crude techniques were devised to aid in the physical recovery of sunfollowers and aspect cameras. The principle involved was to sever the instrument section from the propulsion system on descent from apogee. This destroyed the aerodynamic stability of the rocket and as a result of tumbling through the atmosphere the velocity of the instrument section was reduced sufficiently so that photographic film encased in strong steel cassettes survived the impact.

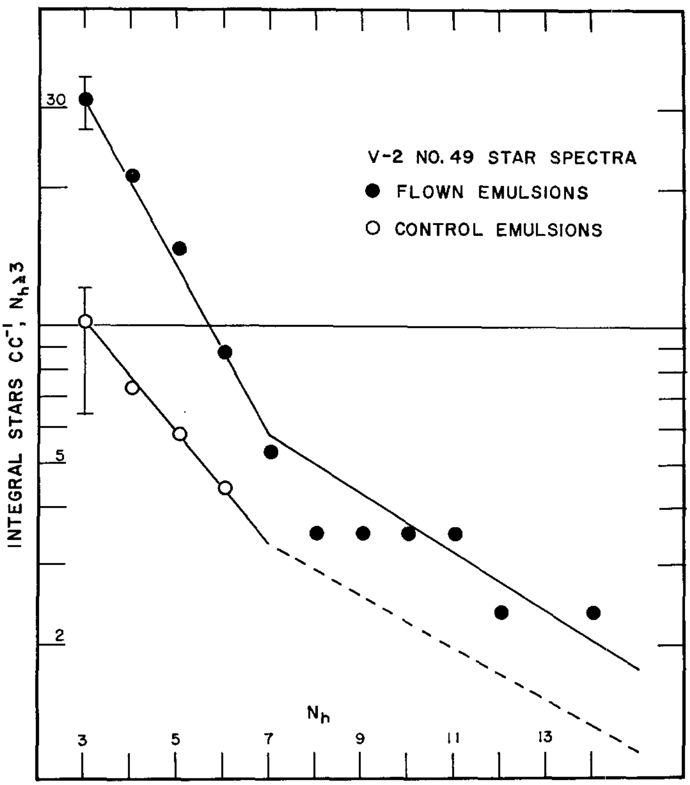

Fig. 1. Star prong spectra on emulsions flown on V-2 no. 49 (A) and control plates (B).

Encouraged by these successful recoveries several cosmic ray laboratories persuing the emulsion technique exposed glass plates coated with 200 micron thick layers of emulsion inside the hollow tail fins of the V-2 rockets. The first of these to be recovered (YAGODA *et al.*, 1950) followed the launching of V-2 No. 49 on 29 September 1949. Despite the brevity of the transatmospheric flight a careful comparison of the rocket exposed plates (Figure 1) with a set of identical manufacture which accompanied the main set to White Sands (ground control plates) showed that the frequency of star production in emulsion could be estimated. Also a few of the then newly discovered heavy primary tracks were recorded, suggesting that if larger areas of emulsion could be exposed in a more favorable geometry it would permit the evaluation of their flux and a clean cut determination of their charge spectrum.

The primative methods of exposure and recovery characteristic of the early V-2, Aerobee and Viking rocket are now largely of historical interest and those of scholarly mind may find reviews of these pioneering efforts culturally rewarding (NEWELL, 1953; ROSEN, 1955; YAGODA, 1957, 1960). This article will concern itself largely with more recent techniques of transatmospheric exposure in which the instrument section is returned by parachute, the low impact velocity permitting the exposure to be conducted in the presence of a minimum of surrounding condensed matter. Exposures of this character can now be obtained with a fair degree of success utilizing Aerobee-Hi and Nike-Cajun rockets as vertical probes up to elevations of about 200 km. These vehicles can be launched from White Sands and Fort Churchill and yield about 400 sec. exposures to essentially pure galactic radiation. Emulsion blocks have been recovered successfully from the 30 min. trajectories of liquid fuel rockets such as the Thor-Able (FREDEN, 1959) and the Atlas (YAGODA, July 1960) thereby providing details on the composition and energy spectra of the trapped radiation at altitudes up to about 1200 km. Exposures of several days duration can be secured by means of recoverable satellites such as the U.S. Air Force Discoverer and the U.S.S.R. space ships. Depending on the apogee achieved, the radiation exposure may be almost purely galactic or an admixture of cosmic, solar and trapped radiations. The polar orbiting satellites sample the complex rediations reaching the earth from all latitudes and longitudes and in order to interpret these results it is necessary to refer to earlier vertical rocket and balloon probe data launched at fixed geomagnetic latitudes. Heretofore unpublished data on Viking rockets Nos. 10 and 11 will therefore be presented in Section VI in order to help evaluate the data from Discoverer No. 35 whose perigee-apogee points overlap the peak elevation reached by the Vikings in 1954.

The nuclear emulsion technique is basically very simple. The recording medium is compact, rugged, adaptable to the diverse shapes and dimensions of the recovery capsule and requires no power for its operation. It has the ability to record and discriminate, as shown in Figure 2, the entire gambit of charged particles from the electron to completely stripped iron nuclei. At low velocities particles stopping in the emulsion can often be identified phenomenologically and their kinetic energies measured with high precision from known range-energy relationships. Particles moving at relativistic velocities can be identified and their energies or momenta estimated by means of the developed grain density, the small angle scattering of the track or the frequency of secondary electrons (delta-rays) associated with the track. This versatility makes the emulsion an invaluable tool for exploratory work on the interplanetary radiations and the unknown phenomena which may still be awaiting discovery as we probe deeper into space.

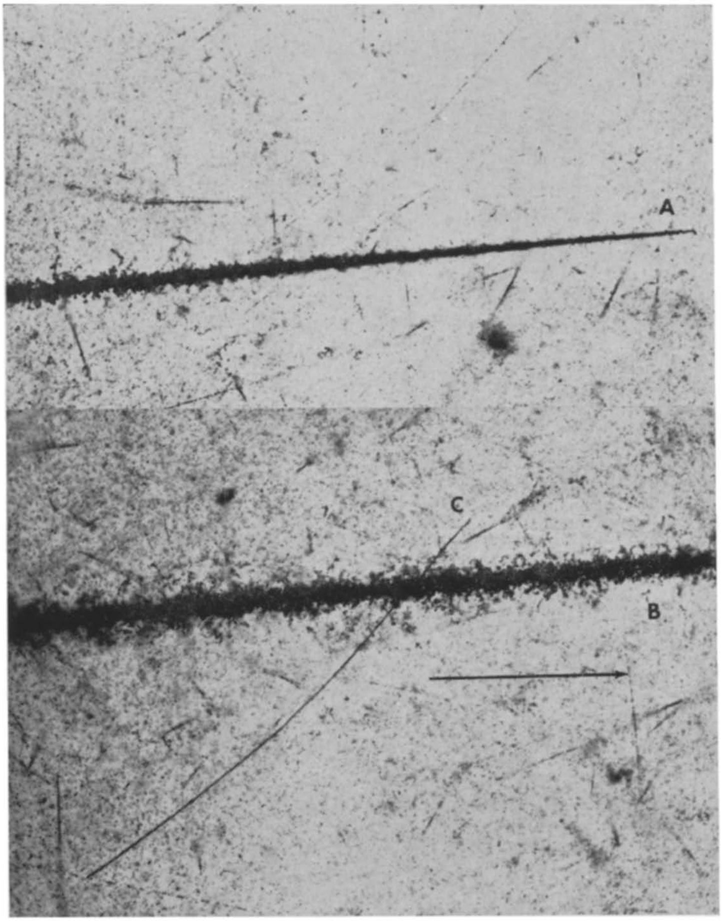

Fig. 2. Photomicrographs of tracks recorded in emulsion block flown on Discoverer no. 32. The heavy tapered track was produced by a particle of $Z = 24 \pm 2$ which comes to rest by ionization at point A. Its maximum of secondary ionization by knock-on electrons is shown at B at 825 ± 25 microns from the terminus. A stopping proton track in the same focal plane is shown at C. The arrow length defines 100 microns.

The simplicity of the tool can be deceptive, however, unless the investigator is prepared to develop the emulsion properly following a four-day orbiting exposure and is temperamentally suited to unraveling the maze of tracks the density of whose information can at times virtually reach a high noise level, particularly if the vehicle spent an appreciable part of its orbit in the trapped radiation belt.

2. The Emulsion Technique

It is beyond the scope of this review to enter on the mechanism of track formation and the diverse details of microscopic measurements indigenous to the technique. The text will be addressed to investigators experienced in the exposure of emulsion blocks in balloons. Newcomers into the field will find the early texts of POWELL and OCCHIALINI (1947) and YAGODA (1949) helpful in getting oriented. More recent and comprehensive texts dealing with the emulsion technique are available by DEMERS (1958) and POWELL, PERKINS and FOWLER (1959). Reviews of intermediary length centered on balloon type exposures have been prepared by BEISER (1952), SHAPIRO (1958) and WIDGOFF (1961). The presentation will be limited chiefly to the problems of stack assembly, methods of exposure and development which in general must be more painstaking and flexible than in balloon work in order to cope with the greater accelerative forces, problems of re-entry heating, recovery over the sea and the greater gambit of radiation levels encountered by deep space probes.

The nuclear emulsion is composed of a dispersion of approximately equal volumes of silver bromide in gelatin with minor additions of plasticizer and sensitizing agents. They are prepared on a commercial basis by Ilford Ltd. in London, England, the NIKFI Institute in Moscow, U.S.S.R. and the Eastman Kodak Company in Rochester, New York, U.S.A. Independent of source all tend to maintain the same chemical and atomic composition shown in Table I for the Ilford type G5 emulsion. The medium

TABLE I

COMPOSITION OF STANDARD* G5 EMULSION

Constituent	*Atomic Number*	*Grams Per cc.*	*Atoms Per cc.*
Ag	47	1.8088	101.01×10^{20}
Br	35	1.3319	100.41
I	53	0.0119	0.565
C	6	0.2757	138.30
H	1	0.0538	321.56
O	8	0.2522	94.97
N	7	0.0737	31.68
S	16	0.0072	1.353

* The composition of the standard G5 emulsion is that adapted by BARKAS (1958) for range-energy computations. It has a density of 3.815 g. cm^{-3} at a relative humidity of 60 per cent, and contains a total of 1.0446×10^{24} electrons per cm^3.

can be coated on specially treated glass plates so that layers from 15 to 1500 microns thickness will adhere under normal conditions of pressure and humidity. Coatings on glass are in general difficult to develop uniformly when their thickness approaches 600 microns and the small shock resistance of the glass base reduces the probability of a successful recovery.

The use of glass backed plates has been supplanted, even in balloon work, by unsupported sheets of emulsion often referred to as pellicles as shown at B in Figure 3.

This permits building up the thickness to any desired degree and the homogeneous block greatly extends the utility of the method as tracks of great length can be followed over an increased angle of incidence. The stacks are commonly assembled from 600 micron thick pellicles. On rocket flights of short duration, 1500 micron thick pellicles

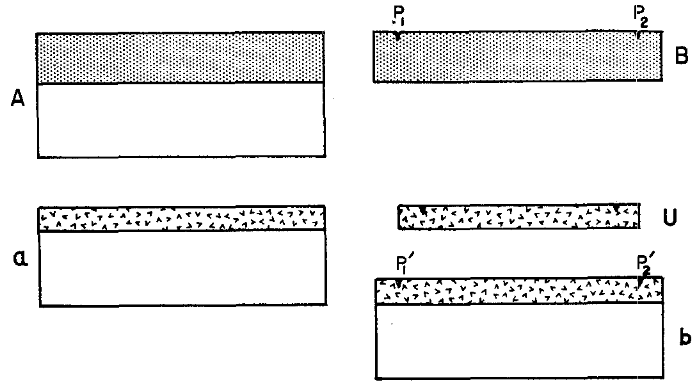

Fig. 3. Comparison of emulsions coated on glass A with stacks of unsupported emulsion layers B. After processing on a glass plate the residual gelatin (a) shrinks only in thickness. Emulsions developed unsupported shrink in area as well as thickness (U). When finally mounted on glass (b) the area is restored to original size by moistening the gelatin sheet until fiducial marks ($P'_1P'_2 = P_1P_2$).

are advantageous as their use simplifies the following of the tracks from sheet to sheet, and when the individual layers are developed so that solutions can reach both faces good uniformity in track structure as a function of depth can be achieved.

When the pellicles are maintained at 50 to 60 per cent relative humidity the preparations can be cut or milled to any desired shape, including circular disks, using dark amber illumination. The cut edges blacken for a depth of several hundred microns owing to the formation of a mechanical latent image by the cutting operation. This factor must be kept in mind in assembling blocks for exposure to very low energy particles. Since the dry emulsion sheets are sensitive to abrasion the surfaces must also be handled carefully in the assembly of the block, an operation facilitated by the generally poor light sensitivity of the nuclear type emulsion. The assembly operation can be conducted under the same level of illumination as commonly employed in enlargement printing work. The abrasive property can be utilized advantageously in identifying the individual sheets with numbers inscribed with a medium soft pencil, and needle points at a known fixed distance P_1 P_2 impart accurate fiducial points on the surface as shown in Figure 3B in restoring the processed sheet to its original areal dimensions.

The component sheets must be assembled into a rigid structure so that the members are accurately aligned. This can be achieved with the aid of plastic clamping plates of adequate rigidity and pre-exposing the back glossy surfaces of the pellicles with a coordinate net (WIDGOFF, 1961). The assembly should be conducted in a dust free room separated from the main processing laboratory. In particular, hypo crystals and metallic filings will cause severe blackening of the emulsions. The unit must be rendered light tight, impervious to chemical vapors and water-tight. In the assembly it must be born in mind that during the trans-atmospheric exposure the package will tend to become evacuated and if the recovery operation is over the ocean salt water will tend to seep in between the voids. This causes fogging of the emulsion and the individual sheets may become bonded if several days elapse between the recovery and the opening of the package at the home base.

Specific instructions cannot be formulated owing to the great diversity of exposures. The problems are rendered particularly difficult as the protective measures tend to counteract the prime objective of maintaining surrounding matter at a minimum. In general, the water-proofing can be accomplished by the use of several layers of thin polyethelene rubberized tapes. The initial layer should be of black polyethelene as this renders the package light tight and facilitates the execution of neat overlapping folds under normal diffuse illumination. The tacky rubberized surface can be placed in direct contact with the emulsion without causing fog. This appears to be a better practice than the use of intermediary black paper, because if water does penetrate, the paper fibers become permanently embedded in the sensitive surface and destroy microscopic visibility, whereas the plastic tape strips cleanly.

Simple taping is adequate for emulsion blocks weighing up to 1 kg. For larger detectors a mechanical clamping device is desirable to prevent the component sheets from buckling and to provide a means of support to the instrument section framework. All direct contact between emulsion and metals must be avoided as electrolytic decomposition can be sep up. Even supposedly chemically inert metals such as stainless steel and aluminum alloys should be coated with a plastic layer or grease film in order to inhibit pseudophotographic action (YAGODA, 1949).

A few cautions concerning the temperature stability of nuclear emulsion will be helpful in reducing chemical fogging during the period between assembly and the highly variable date of large rocket launchings. The block should be kept cool at 3 to 5° C in a refrigerator located at great distances from radioactive sources and X-ray machines. Since the sensitivity is reduced with diminishing temperature large blocks of emulsion should be removed from the refrigerator about 10 hours prior to scheduled launch time for thermal equilibration of the component pellicles. At temperatures below the freezing point the sheets tend to become brittle. The highly sensitive G5 emulsion will retain some sensitivity for densely ionizing particles even at liquid air temperatures. As an upper limit the temperature ideally should not exceed about 40° C. Often the launching schedule is delayed and the instrument section may be exposed to intense sunlight for several hours. This situation can be counteracted by a flow of cool air. The numerous temperature changes taking place while the vehicle is in orbit and re-entry does not appear to be a cause of excessive chemical fogging. On several occasions small disks of emulsion located outside of the capsule, but beneath about 2 g. cm^{-2} of ablation material have been recovered after 1 to 4 days in polar orbit without appreciable greater fogging than observed in emulsion located inside the protective capsule.

After recovery the emulsion should again be kept cool whenever feasible. A crude storage box constructed from 3 cm thick slabs of styrofoam is useful. It is particularly effective when used in conjunction with several cans of frozen orange juice which serves as a thermal sink, and often helps preserve the experimentalist as well as the emulsions on difficult desert recoveries. In returning the emulsions to the laboratory thought should again be given to external radiation sources. Wrist watches with luminous dials should be avoided. Likewise a rear seat in airplanes should be selected as the large number of radioactive dials in the plane's cockpit constitute an appreciable gamma ray source (YAGODA, April 1961).

3. Geometric Aspects of the Exposure

A. SOLID ANGLE EFFECTS

The emulsion is an omnidirectional detector of continuous sensitivity hence in a vertical rocket probe or in an elliptical satellite orbit radiation reaching the emulsion at an angle θ with the vertical will traverse varying air masses $m\ (\theta, h)$ with variations in the elevation above the earth's surface, h. When h is small, as in balloon exposures, the earth shadows the lower part of the detector and

$$m\ (\theta) = m_0/\cos\theta \tag{1}$$

is a good approximation up to $\theta \leqq 75°$ where m_0 is the vertical air mass. At rocket elevations the situation is more complex, for as shown in Figure 4 in the absence of an

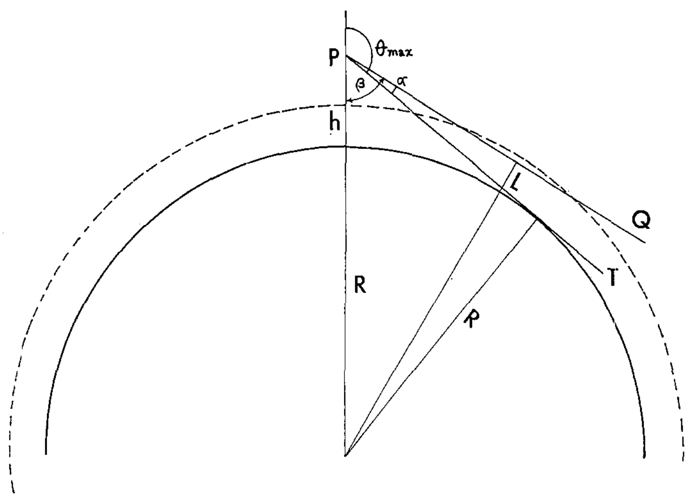

Fig. 4. Geometry for computing the air mass traversed by radiation at detector P at an altitude h above the earth's surface.

atmosphere a ray T can reach the detector at point P over a maximum angle θ_{max} such that

$$\sin\theta_{max} = R/(R+h) \tag{2}$$

where R is the radius of the earth. Owing to the presence of the atmosphere ionizing particles can only reach the emulsion without suffering attenuation either by collision or ionization processes over a more restricted angle π-β and a small penumbral angle $\propto$ will exist at large values of h which will permit some of the more energetic particles to penetrate from the lower hemisphere.

Neglecting ionization loss, but considering a beam of particles of attenuation length L in a given medium it can be shown (ROSSI, 1952) that the effective solid angle $\bar{\omega}$ at a vertical depth m_0 is:

$$\bar{\omega}(m_0) = \left[\int J(m_\theta)\, \mathrm{d}\omega \right] / J_v(m_0)\,, \tag{3}$$

where
$$J(m_\theta) = J_v(m_0) \exp \{-(m_0/L)[(1/\cos\theta - 1)]\}\,, \tag{4}$$

and
$$J_v(m_0) = J_0 \exp(-m_0/L)\,, \tag{5}$$

and
$$\int J(m_\theta)\, \mathrm{d}\omega = 2\pi m_0 J_0 \int_{m_0}^{\infty} \frac{\exp(-m_\theta/L)}{m_\theta^2}\, \mathrm{d}m\theta\,. \tag{6}$$

Equation (6) is commonly referred to as the GROSS transformation.

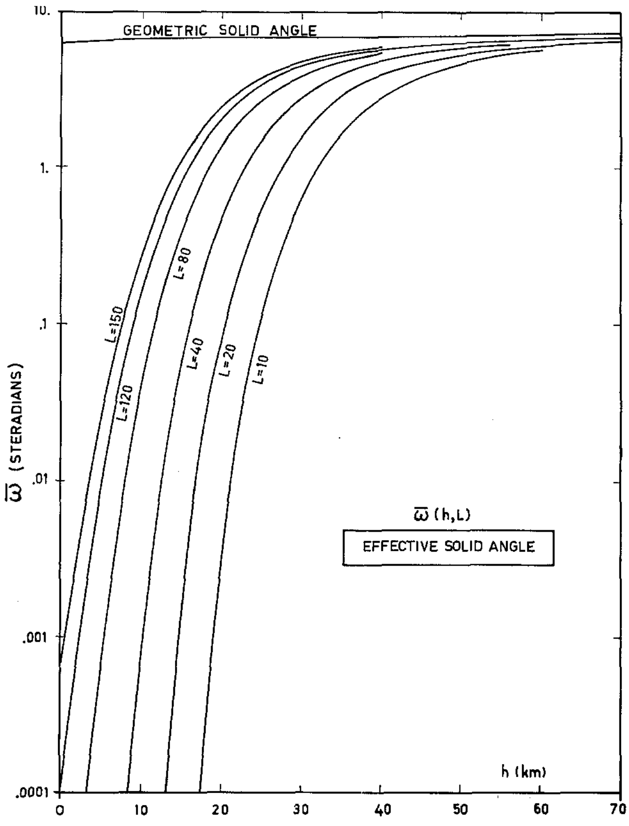

Fig. 5. Variation of the effective solid angle with altitude and collision mean free path in air.

Values of m_θ for elevations up to 150 km have been computed by PRESSLY (1953) using the Rocket Panel standard atmosphere of 1952. More recently, the problem has been re-examined by ELY (1962) who has computed values of m_θ from sea level up to 680 km using the density data of the ARDC 1959 Model Atmosphere. ELY has also computed $\bar{\omega}(h, L)$ using values of L from 10 to 150 g. cm^{-2} which covers the mean collision path of protons and heavy primary nuclei in air (Figure 5) and tabulates values of the integral

$$\bar{\omega}(h, L) = 2\pi \int_0^{\theta max} \exp\left[-m(h, \theta)/L\right] \sin\theta \, d\,\theta \,. \tag{7}$$

The report also treats of a more general effective solid angle $\bar{\bar{\omega}}(h, L, k)$ taking into account the ionization loss parameter k which is significant for non-relativistic particles.

Upper air rocket probes provide exposures of about 10 minutes duration. As shown in Figure 6, the trajectory is essentially parabolic, when expressed in terms of altitude

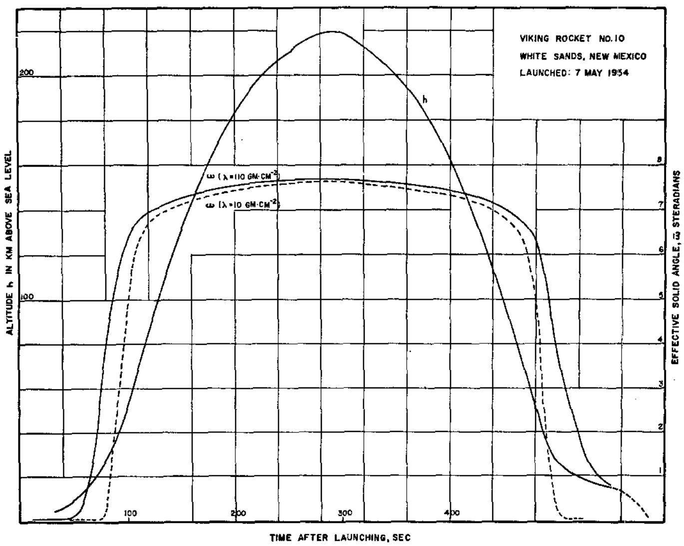

Fig. 6. Trajectory of Viking rocket No. 10 and translation of altitude into effective solid angles.

as a function of time. However, if the altitude is converted into an effective solid angle viewed by the detector it is seen that the exposure assumes a monotomic plateau. In the case of the Viking No. 10 flight, used for illustrative purposes, heavy primary nuclei of $Z \geqq 20$ could reach the emulsion over an effective solid angle $\geqq 2\pi$ steradians for 360 sec or 62 per cent of the flight time. On a balloon flight reaching a 40 km ceiling plateau the effective solid angle is limited to 2 steradians.

Thus far only a bare point detector has been considered devoid of any surrounding condensed matter. When the emulsion block is embedded inside a crowded instrument section the real solid angle $\bar{\omega}_c(h, L_c)$ is in general more difficult to evaluate as it is necessary to carry out a numerical integration of the complete absorber paths through air and condensed matter. Often the computations can be simplified by assuming that the emulsion is surrounded by an uniform shell of thickness t g. cm^{-2} in which the particular radiation has a collision mean free path of L_c g. cm^{-2}. The corrected effective solid angle is then approximated by

$$\bar{\omega}_c = \exp\left(-\, t/L_c\right) \bar{\omega} \,. \tag{8}$$

In the Viking No. 10 exposure shown in Figure 6, t was 2 g. cm^{-2} of aluminum and L_c for nuclei of $Z \geqq 10$ is 27 g. cm^{-2}. At the apogee of 220 km, $\bar{\omega} = 7.7$ steradians and this becomes reduced to $\bar{\omega}_0 = 7.15$ steradians as a result of the presence of the nosecone and the heavy walled aluminum cassette.

In employing rocket probes for the study of radiations having small collision paths it is essential to keep the value of t at a minimum. In the more recent geophysical rockets the nosecone can be jettisoned at about 50 km and since the instrumentation is brought back by parachute the emulsion housing thickness can be reduced to about 0.2 g. cm^{-2}. The effect of these improvements is compared in Figure 7 for an Aerobee rocket above the atmosphere, A with the nosecone in place and B after nosecone ejection.

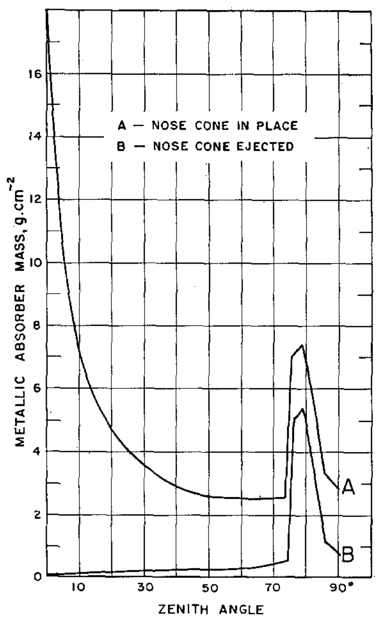

Fig. 7. Dependence of metallic absorber mass on zenith angle of incident radiation for Aerobee exposure described in Figure 12.

In early studies of the nucleonic component with Aerobee and Viking rocket probes the effective time of flight was arbitrarily taken as the interval above 30 km altitude. This was convenient in order to compare the results with those measured at balloon elevations (YAGODA, 1956). With the advent of multistage rockets and their penetration into the trapped radiation belts it has been proven more useful to base the exposure time on the period spent in the vicinity of apogee. The average altitude $\bar{h}$ of a vehicle that follows a parabolic trajectory of peak elevation H is:

$$\bar{h} = 2H/3 \tag{9}$$

The effective exposure can therefore be considered as the time interval over which $h \geqq \bar{h}$ and an accurate flux can be evaluated for an altitude region between H and $\bar{h}$ having an average value of $8H/9$ provided correction data is available to the $\bar{h}$ level. This approach is particularly useful in the interpretation of data from a multiple exposure such as the galactic and trapped Van Allen radiations where the intensity of the latter increases very rapidly with elevation. Typical exposure periods for high altitude vertical probes are shown in Table II.

TABLE II
FLIGHT CHARACTERISTICS OF VERTICAL ROCKET PROBES

Vehicle	*Elevation, km*		*Exposure Period sec.*	
	H	$\bar{h}$	$\geqslant 30\ km$	$\geqslant \bar{h}$
Aerobee	124	82	286	192
Aerobee-Hi	193	129	357	240
Viking 9	217	144	407	248
Viking 10	219	146	414	260
Viking 11	255	170	457	279
Nike-Cajun	122	81	300	182
Atlas, July 59	1177	784	1800	980
NERV	1884	1260	~2300	~1400
Scout D-5	1875	1250	2280	1390

Prior to the discovery of the trapped radiation belts and the launching of orbiting satellites it was felt that the brief exposures secured by the small geophysical rockets could be extended through the use of more powerful vertical probes. Since the exposure period increases slowly as $H^{1/2}$ this was a difficult approach to long duration trans-atmospheric cosmic ray exposures. The situation is further complicated by entry into a more intense radiation level at elevations $\geqq$ 500 kms. The large background of trapped protons encountered during a 30 min. Atlas rocket flight severely limits the ability to study the galactic radiation. As shown in the photomicrograph of an emulsion recovered from an Atlas trajectory, Figure 8, the heavy cosmic ray primaries can be discerned, but the intense proton track background prevents the ready discrimination of tracks produced by particles of lesser ionizing power.

Unshielded exposures at elevations in the region of 2000 km would yield excessively blackened emulsions. Greatly extended exposures to essentially pure galactic radiation are best achieved by means of recoverable satellites whose apogees do not exceed 300 km. Exposures of this character have been obtained by ALEKSEEVA in the second Soviet Space Ship launched August 1960 and by YAGODA on Discoverer 35 launched into a polar orbit of 306 km apogee on 15 November 1961.

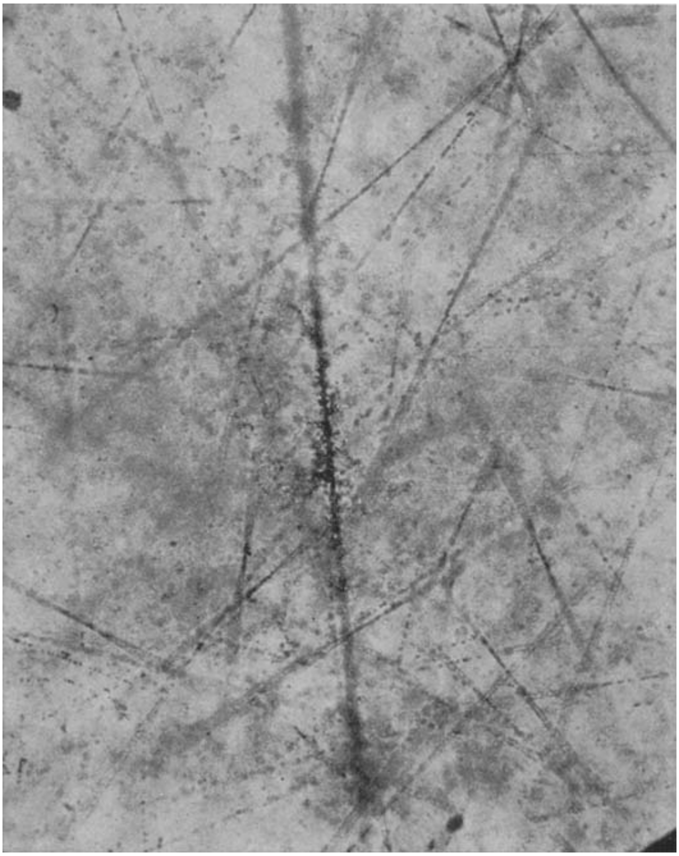

Fig. 8. Photomicrograph from an emulsion recovered from the Atlas flown 21 July 1959 showing a heavy primary track against a background of trapped protons.

B. GEOMAGNETIC FIELD EFFECTS

Charged particles approaching the top of the atmosphere are deflected by the earth's magnetic field. Particles with momenta in excess of r Störmer units approaching at a zenith angle θ and an azimuthal angle ϕ will reach a point of geomagnetic latitude λ, provided

$$r = \cos^2 \lambda / [1 + (1 - \sin\theta \cos\phi \cos^3 \lambda)^{1/2}] \,. \tag{10}$$

For a detector at an elevation $R + h$ above the earth's center the cutoff energy for protons E_p is:

$$E_p = 0.939 \left[\left(\frac{1 + 6.77 \times 10^{38}\, r^4}{(R+h)^4} \right)^{1/2} - 1 \right] \text{Bev} \,. \tag{11}$$

For multiply charged particles of A = 2Z, the energy per nucleon ε_0 is related to E_p as follows:

$$\varepsilon_0 = [(E_p^2 + 1.87\, E_p)/4 + 0.872]^{1/2} - 0.939 \text{ Bev/nucleon} \,. \tag{12}$$

In detectors flown at balloon elevations where the field strength is not reduced appreciable $R + h \simeq R$, but at the greater elevations reached by rockets and satellites the cutoff energies are sensitive to h. The effect of increasing altitudes on the cutoff energy for protons incident vertically at the geomagnetic equator is shown in Figure 9.

For an omnidirectional detector, such as an emulsion block measuring the star producing radiation the situation is complicated by the strong dependence of r on direction of arrival. In order to interpret star data secured on rocket flights launched from White Sands, New Mexico ($\lambda = 41°$ N) the average flux of primary protons $\bar{j}(\theta)$ integrated over $\phi = 0$ to 360° has been computed as a function of h, assuming as a model that

$$j = \frac{5000}{(1 + E_p)^{1.5}} \text{ particles per m}^2\text{. sec. sterad .} \tag{13}$$

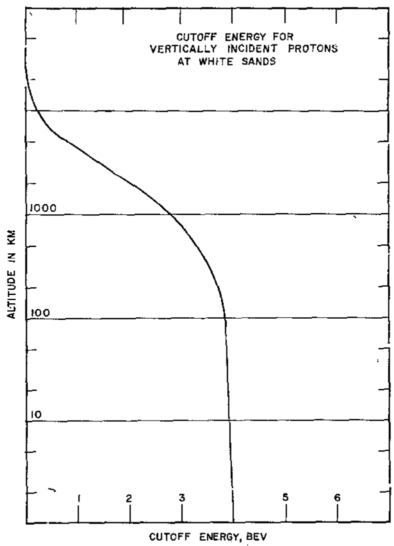

Fig. 9. Variation of cut-off energy for protons as a function of altitude.

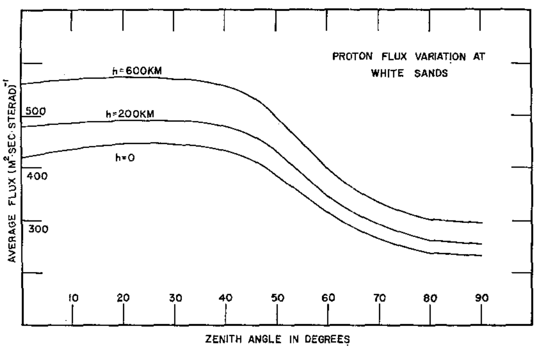

Fig. 10. Variation of proton flux averaged over all azimuthal angles as a function of zenith angle and altitude.

Using values of r computed by Alpher (1950) which take into account the Störmer plus the earth's shadow cone at $\lambda = 40°$ the variation of $\bar{j}$ with θ is shown in Figure 10 for elevations up to 600 km. The average flux $\bar{j}$ integrated over all zenith and azimuth angles increases 28 per cent between 0 and 600 km elevation. For exposures in satellites launched into polar orbits similar curves of $\bar{j}(\theta, h)$ should be available for all geomagnetic latitudes. Alpher's values of the Störmer unit, however, are based on a dipole moment for the earth's magnetic field, a model which is now known to be an oversimplification. For approximate purposes of comparing satellite measurements with geomagnetic theory, the $\lambda = 40°$ functions can be used as a rough average for the energy cutoffs between the equator and the poles.

4. Exposure Mechanisms

The exposure of nuclear emulsion blocks in space probes can be described under two broad categories – static and dynamic. In the static exposure the block remains fixed with reference to the frame of the instrument section and does not permit any time resolution in the passage of individual particles. Figure 11 of the instrument section

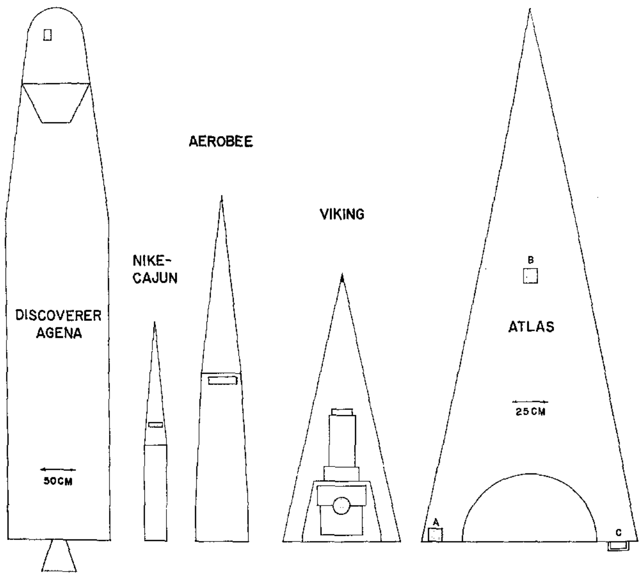

Fig. 11. Comparative dimensions of instrument sections on geophysical sounding rockets and Discoverer Agena, the latter drawn to 1/2 scale of the other instrument sections. The shaded areas represent the position of emulsion blocks. An attempt was made to sample on the outside of the Atlas block, position C, by covering the emulsion with a 1 cm layer of ablation. The unit survived reentry, but was lost during the sea recovery operation.

flown on Viking rocket No. 10 is an example of the better type of exposure secured before parachute recovery techniques were perfected. In the dynamic exposure chronologically correlated movements of the emulsion components provide a measure of the time at which particles entered the detector and hence the altitude of recording.

A. STATIC EXPOSURES

In general, the small emulsion blocks weighing less than 1 kg can be flown in conjunction with other geophysical upper air experiments where physical recovery of the equipment and ejection of the nose cone is essential. A good example of this collaborative type of exposure is shown in Figure 12. By polishing the surface of the emulsion cassette high velocity impacts by meteoritic dust can be detected by microscopic and contact printing methods of analysis (YAGODA, May 1957). The upper surface of the aluminum cassette was 0.4 mm thick, and including wrapping materials the layer of condensed matter was only 0.14 g. cm^{-2} (YAGODA, July 1958). Similar

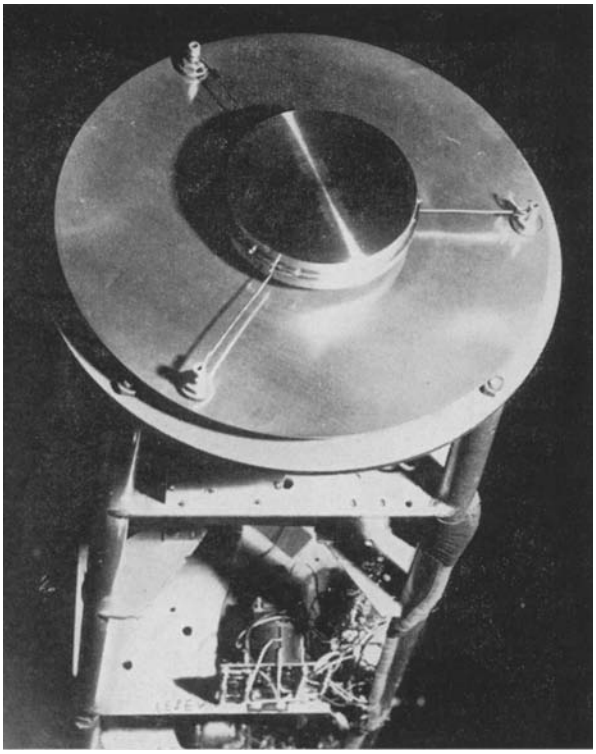

Fig. 12. Exposure of emulsion cassette in conjunction with a micro-meteorite experiment.

static exposures can be secured on vehicles designed to study the airglow and auroral spectra (Figure 13).

A similar static exposure, although the block was mounted on a moving sun-seeking spectrograph is shown in Figure 14. Here the nose cone is not ejected, but a panel is blown off when the rocket is above 50 km permitting the spectrograph to extend at a large angle with the longitudinal rocket axis. An emulsion block measuring 10×15 cm and weighing about 500 grams can thus be given a free space exposure over 2π steradians with a local absorber mass over the first sheet of 0.1 to 0.2 g. cm^{-2}. Prior to severing the motor section the spectrograph is retracted into the nose cone which offers additional protection in the final parachute landing.

Another example in which the emulsion block is an inert passenger on moving parts of the rocket frame is shown in the Venus Flytrap Nose Cone designed for the collection of meteoritic dust (SOBERMAN, 1961). The nose cone Figure 15 is fired in the fully closed position. An electric motor then raises the outer skin at about 90 km. A second motor aided by 2 rps spin applied to the rocket extends the eight collector arms on which it is possible to mount small emulsion blocks ($\leq$ 200 grams) covered by light tight foils weighing about 0.05 g. cm^{-2}. After reaching apogee the leaves are retracted starting at an elevation of about 140 km. This is facilitated by de-spinning the free

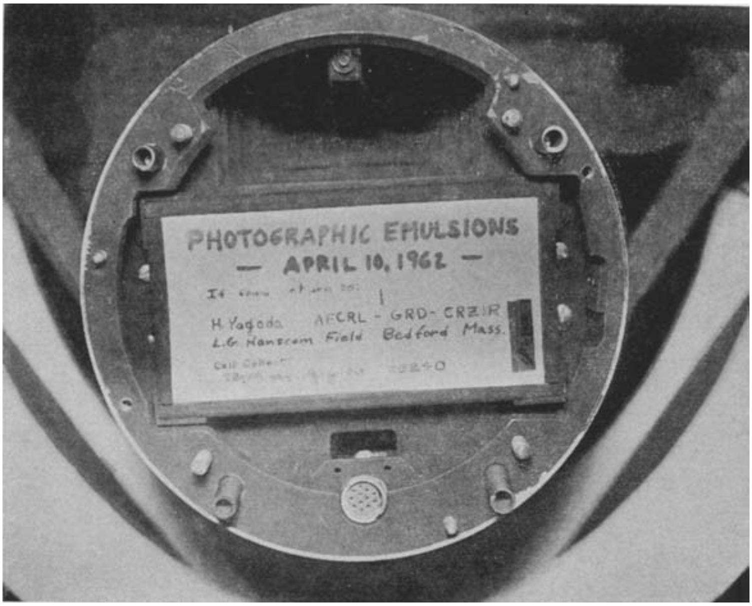

Fig. 13. Orientation of emulsion block on Aerobee rocket designed to study auroral spectra.

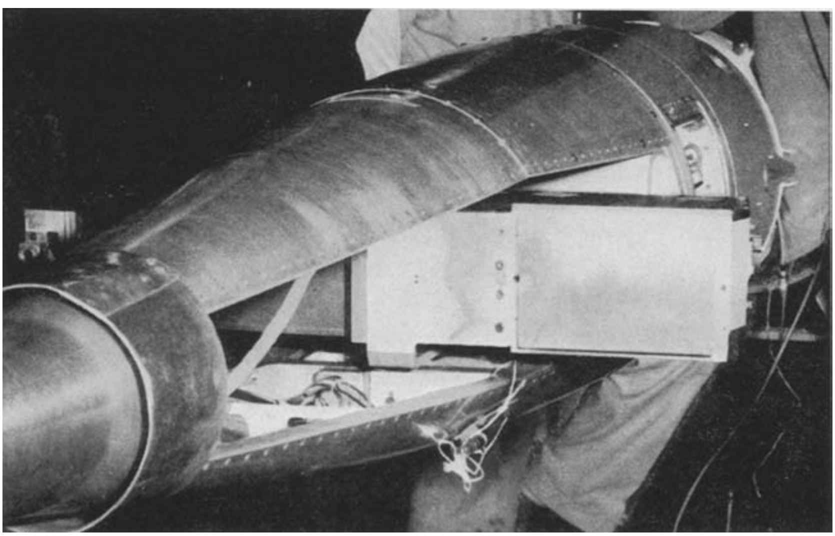

Fig. 14. Emulsion block mounted on spectrograph oriented by a sunfollower.

falling rocket which also reseals the unit to prevent entry of atmospheric dust. The booster section is then severed from the payload and finally a parachute was deployed at 6 km altitude. Using an Aerobee which reached a peak altitude of 168 km a free space collection period of 236 seconds was achieved.

Utilizing motor driven rack and pinion movements emulsion blocks can be extended through the skin of the instrument section, thereby securing an exposure with a diminished background of secondary radiation. The primary radiation interacts with the massive rocket body and the secondary evaporation particles reach the emulsion detector with an intensity which diminishes roughly with the square of the distance between the block and the center of gravity of the vehicle. Fortunately, the greater

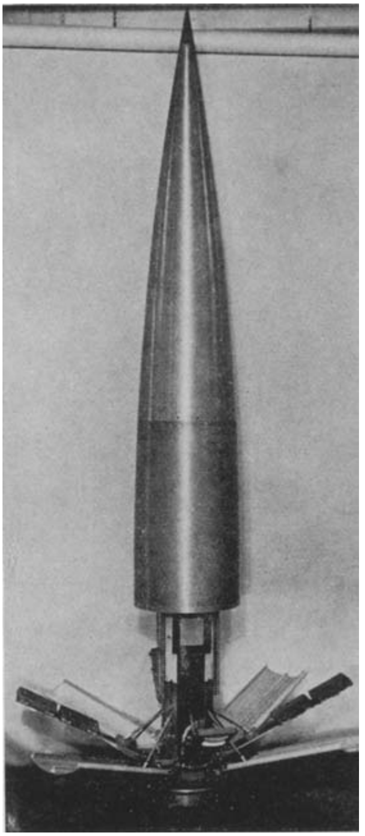

Fig. 15. Aerobee nosecone designed for the collection of meteoritic dust. Some of the pockets can be fitted with small emulsion blocks.

part of the rocket mass is lost during the early stages of ascent. As a consequence the major fraction of the secondaries are created mainly in the instrument section which constitutes only a small fraction of the total mass of the vehicle.

On the Viking rockets the base of the conical instrument section had a diameter of 114 cms, permitting the extension of an arm about 1 meter long. A "baker's paddle" designed to extend a five pound block of emulsion was constructed for exposure on Viking No. 13. Owing to its transfer to the Vanguard satellite launching program this rocket was launched from Cape Canaveral where recovery in water was not feasible. Smaller versions of this extension-arm can be adapted to more compact geophysical sounding rockets. A small spring-driven arm designed for the collection of meteoritic dust is shown in Figure 16. The triangular prism section supports glass slides. These can be replaced with a sheet of emulsion covered with black polyethylene tape. Over a limited solid angle the condensed matter absorber path is only 0.020 g. cm^{-2}. This permits the detection of 3 Mev protons and alpha particles whose kinetic energy exceed 10 Mev.

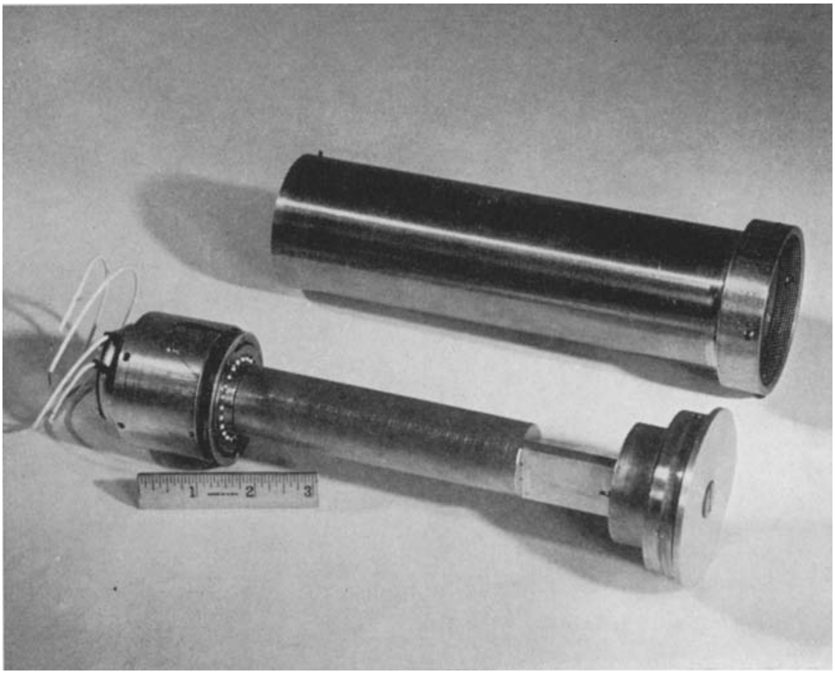

Fig. 16. Extension arm for the collection of meteoritic dust and the exposure of emulsion pellicles under near free space conditions.

In several respects the Nike-Cajun vehicle offers several advantages over more massive vehicles, as after burnout of the second stage the dead weight accompanying the experiment is only about 44 kg, roughly one-third that of the Aerobee. The Nike instrument section, however, is only 16 cm in diameter as compared with the 38 cm diameter of the Aerobee. This limits the size of an emulsion block to a square of about 10 cm edge. With a minimum payload of 11.3 kg the vehicle when launched vertically reaches a theoretical peak elevation of 225 km some 240 sec after firing. The Nike-Cajun sounding rocket fitted with a parachute recovery system has been employed extensively by FICHTEL (1961, 1962) in studies of the composition of the charged particles emitted during solar flares. Altitudes of about 120 km have been achieved, and an 85 lb payload can be carried to 130 km (BISWAS, 1962). While the exposure period of 400 sec is small, the intensity of the solar radiations are several thousand times greater than the normal galactic background and data of good statistical weight can be secured. The recovery of the equipment from the difficult Fort Churchill terrain has been phenomenally good; in about two-thirds of the firings the payload has been retrieved. A method of exposure to low energy solar protons devised at the Geophysics Research Directorate is described in Figure 17.

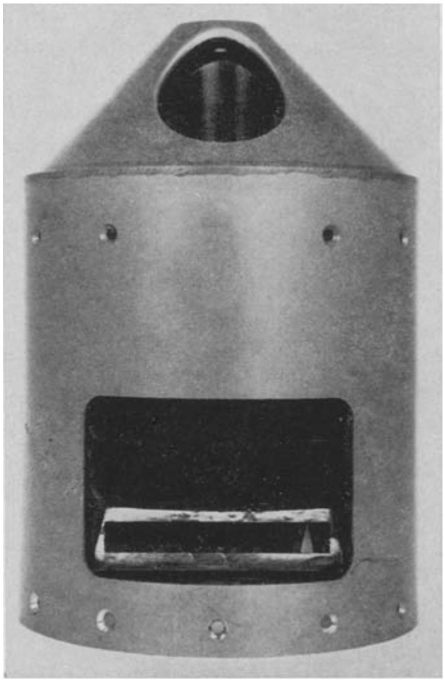

Fig. 17. Exposure of 10 × 10 × 2.5 cm block of emulsion in a Nike-Cajun nosecone. The block can be rotated so that two of the 10 × 2.5 cm sides face an opening in the rocket skin during flight above 50 km. These faces contain vertically oriented sheets of emulsion which permit the detection of protons with a minimum energy of 4 Mev.

In 1957 GROETZINGER organized a committee for Extra-Atmospheric Cosmic Ray Research which made a feasibility study of the launching of large blocks of emulsion to high altitudes. With the Vanguard type propulsion systems available at the time it appeared possible to expose 23 kg of nuclear emulsion for approximately 35 min. in a near vertical trajectory with an apogee of 2880 km. The discovery of the intense trapped radiation belt at altitude $\geqq$ 600 km and the concurrent launchings of recoverable satellites with apogees $<$ 600 km were largely responsible for the abandonment of this high altitude shot. However, the design proposal assembled by the Martin Company (October 1957) contains numerous novel features for the exposure and recovery of emulsions worthly of further study as a mean of determining the particle composition of the radiation belts utilizing less sensitive emulsions than contemplated at the time.

Emulsions have been exposed for periods of 1 to 4 days in recoverable satellites launched in the U.S.S.R. and from Santa Maria, California. A longitudinal view of the Discoverer capsule showing the orientation of diverse emulsion blocks is shown in Figure 18 relative to the position of other metallic components whose activity has been measured after concentration by radiochemical techniques (FIREMAN, 1961). The exposures are of the static category, and the position of the blocks have been varied, within the limitations of available space, to take advantage of reduced absorber masses. The block at E is composed of 20 sheets of emulsion measuring 10 × 15 cm and 600 microns thick weighs about 750 grams. The sensitivity of the sheets are

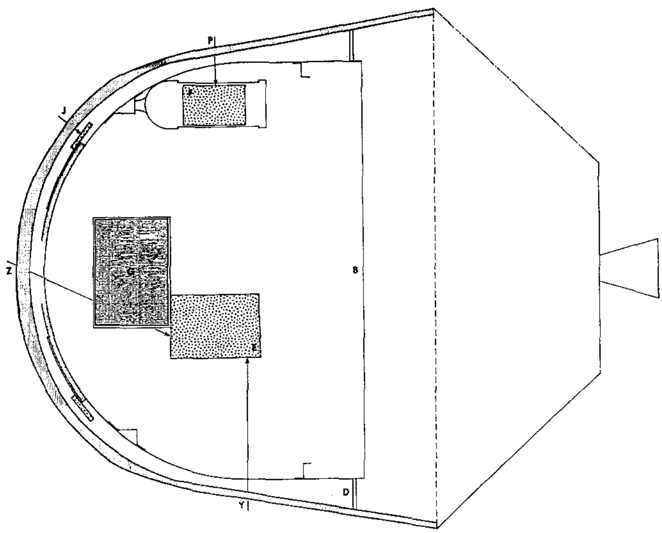

Fig. 18. Longitudinal section of Discoverer capsule showing positions of emulsion blocks and metals exposed in polar orbit. Emulsion blocks at position E, F and J have absorber paths of $Y = 2.8$ g.cm^{-2}, $P = 2.2$ g.cm^{-2}, $Z = 4.7$ g.cm^{-2} and $J = 1.89$ g.cm^{-2}. The thin-wall aluminum capsule B is supported against the outer ablation material by a 6 mm thick aluminum flange D. The emulsion disks J below the ablation are supported on a 6 mm thick lead ballast. The stainless steel on the storage battery G is useful for tritium-argon analyses.

varied from the most sensitive Ilford G5, and include the finer-grained K5 and L4 types to be in a position to cope with a variety of exposure periods and altitude dependent radiation dosages. Small circular disks of emulsion have been mounted in watertight stainless steel cassettes in position J on the outside of the capsule but beneath the heat shield. Each cassette contains 5 circular disks of emulsion 47 mm in diameter and 600 microns thick. While the collecting volume is small the detector has a 2π steradian view obstructed by only 1.89 g. cm^{-2} of condensed matter including the aluminum cassette cover. More recently several small rectangular slabs of emulsion have been exposed on the flange D where the ablation material is about 1 g. cm^{-2}.

The Discoverer satellite follows a polar orbit sampling radiations at all latitudes and a large fraction of the longitudinal surface, as shown in Figure 19. Since the exposures are static an integrated value of the radiations is recorded. Nevertheless, by comparing the average values as a function of vehicle apogee (Table III) important information has been secured on the altitude dependence of the total nucleonic component, and on the proton fluxes in the very lowest fringes of the Van Allen belts. The small emulsion disks J have proven invaluable for measurements of the flux of slow heavy primaries with energies per nucleon $E_0 \geq 80$ Mev. With the maturing of these complex recovery vehicles it should ultimately be possible to provide hinged cut-outs in the heat shield through which emulsions can be exposed to essentially free space environment.

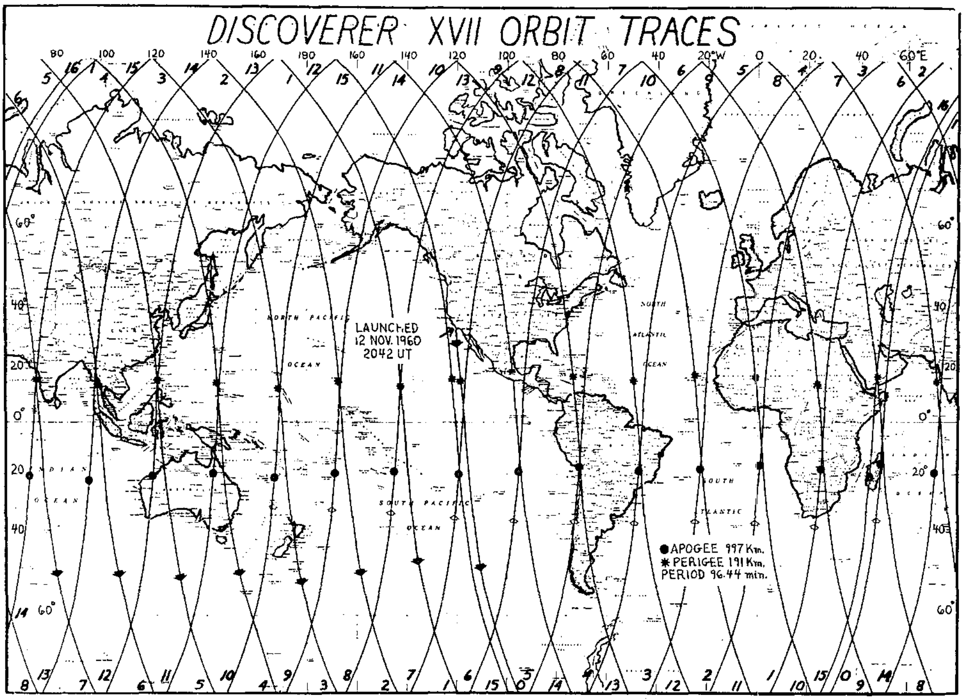

Fig. 19. Map showing the first 16 orbits executed by the Discoverer 17 satellite.

TABLE III
ORBITAL PARAMETERS OF DISCOVERER SATELLITES

Vehicle	Altitude, km		Period min.	Date of Launch	Exposure, days	
	Apogee	Perigee			Total	$\geq 55°$
17	997	184	96.44	12 Nov. 60	2.09	0.77
18	704	246	93.67	7 Dec. 60	3.14	1.22
25	412	224	90.88	16 Jun. 61	2.10	0.78
26*	814	230	95.02	7 July 61	2.13	—
29	563	151	91.55	30 Aug. 61	2.11	0.81
30	579	232	92.41	12 Sept. 61	2.13	0.78
32	405	232	90.85	13 Oct. 61	1.15	0.42
35	306	247	89.84	15 Nov. 61	1.14	0.42
36	502	243	91.85	12 Dec. 61	4.07	1.51

* Vehicle No. 26 had no emulsion on board, but its metallic components were subjects of study because of the long exposure to trapped radiation.

Blocks of nuclear type emulsions have also been exposed on board the Soviet recoverable space ships. ALEKSEEVA and co-workers (1961) mounted a small stack of NIKFI-ER emulsions on the second space ship launched August 1960. The exposure was at an average altitude of 320 km and the flight of approximately 24 hours sampled the radiations between latitudes 0 to 65°. The emulsions, employed in a heavy primary charge study, were exposed beneath 8 g. cm^{-2} of condensed matter. The large Soviet recovery vehicles in principle have room for sophisticated exposures. VEPRIK *et al.*, (1961) describe methods for limiting the exposure period of emulsions carried on board the second spaceship. In one of their approaches, after exposure for a desired period the emulsion is developed and stored in a solution which preserves the silver image but inhibits the further production of latent images. The final fixation, washing, etc. was completed in the laboratory after re-entry from orbit. This preliminary experiment demonstrated the possibility of limiting the exposure to a small fraction of time in orbit.

B. DYNAMIC EXPOSURES

In the more sophisticated dynamic type of exposure the components of the emulsion assembly can slide or rotate with respect to each other so that the position of the recorded tracks are correlated with the time-altitude performance of the vehicle. One of the first of these moving plate devices was exposed by SHAPIRO and STILLER on Viking No. 9 launched 15 December 1952. The apparatus consisted of two glass coated plates separated by an air-gap, one of the plates being supported on a sheet of steel and the other facing an electromagnet. On a command signal the activated magnet brought the two sensitive surfaces in contact, and a second signal would again cause their separation. After development the two recording layers were mounted in register and viewed simultaneously under the microscope. Charged particles which traversed the detector in the closed position, during a select portion of the flight, could thus be differentiated from the random background by linear alignment of the track sections in the adjoining sensitive layers. This device did not withstand the rigors of the high velocity impact characteristic of the Viking recovery operation. However, the basic design should prove practical with modern parachute techniques, particularly if pellicles mounted on plastic are substituted for the fragile glass backed plates.

In an effort to study the time variation in the arrival of cosmic ray heavy nuclei LORD and SCHEIN (1950) devised an apparatus in which two contacting emulsions are moved at an uniform rate with respect to each other, thus permitting an estimate of the time at which a given heavy nucleus traversed the ensemble. A detailed study of the moving plate technique by YNGVE (1953) showed that a rate of motion of about 250 microns per hour was sufficient to determine the time of recording of a particle to within an uncertainty of a few minutes during a balloon flight of 11 hours duration. This mechanism for determining the time history, and hence the altitude, of cosmic ray traversals can also be adopted to shorter rocket flights of 5 to 30 minutes duration by suitable adjustment of the rate of motor speed.

Methods for rotating circular disks of emulsion, in efforts to study the altitude dependence of the flux of trapped protons, have been described by FREDEN (July 1960) and NAUGLE (1961). The nuclear emulsion research vehicle (NERV) flown to a peak elevation of 1884 km on 19 September 1960 represents the first dynamic type exposure in which the entire rocket system was designed for the particular needs of the radiation exposure. The NERV basic payload measures 107 cm and the cylindrical portion has a diameter of 48 cm. The 41 cm aluminum recovery vehicle including the ablation heat shield and experimental equipment weighed 38 kg. A stack of 25 nuclear emulsions 15 mm thick and 76 mm diameter were mounted inside of a cylindrical tungsten shield 1.59 cm thick which had a 1 cm^2 window covered with a 100 micron thick aluminum foil. This aluminum seal maintained the emulsions at sea level pressure during the flight and prevented access of sea water during recovery. The emulsions were nicked around their peripheries and these marks were aligned with the window and with a marked disk on top of the stack. At an altitude of 480 km a small electric motor extended the tungsten shield 83 mm beyond the nose cone, and retracted the apparatus at 960 km during the descent. During this period a chronometrically driven motor rotated the emulsions one revolution. A point on the emulsion periphery was behind the window for 80 sec and was subsequently shielded by 30.6 g. cm^2 of tungsten. The shielding stopped protons with kinetic energies up to 150 Mev. Radiation entering the window permitted a measurement of the lower end of the spectrum down to

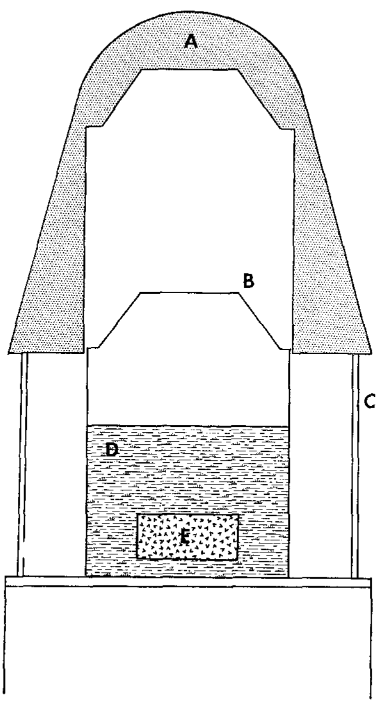

Fig. 20. Instrument section of the Scout D-5 vehicle with reentry ablation shield A in extended position. The emulsion block E is embedded, with other instruments in a unicellular plastic foam, sealed inside a 1 mm thick aluminum shell.

energies of 8 Mev. The first launching was successful in every respect and after a total flight of about 37 minutes the capsule was retrieved after only about 2½ hours in the water. Since then, two additional launchings have been unsuccessful in the recovery operation.

Another attempt to study the trapped and cosmic radiations in a high altitude probe was made by YAGODA and SHAPIRO who exposed a $15 \times 15 \times 6$ cm block of emulsion weighing 8 kg in the instrument section (Figure 20) of Scout vehicle D-5. The solid propellant rocket was launched from Cape Canaveral on 12 April 1961. After second stage burnout the primary heat shield was separated thus exposing the sealed recovery unit. The re-entry ablation cone A is extended above the instrument package B by means of a pair of pneumatically operated telescoping tubes C, thereby allowing radiation to reach the sides of the emulsion block E embedded in plastic foam D with a shielding of 0.76 g. cm^{-2}. Prior to re-entry a second set of pneumatically operated tubes reinsert the canister B into the cavity of the recovery vehicle nose cone. The nose cone reached an apogee of 1874 km, but was lost at sea.

5. Emulsion Development

The standard method of premounting the exposed pellicles on glass prior to processing with amidol developer is generally suitable for emulsions exposed in rocket probes of 5 to 30 minute duration. With longer exposures, accompanied by deeper penetration into the Van Allen belts, it is necessary to weaken the strength of development in order to avoid excessive blackening. Also, because of the nature of the recovery involving high rates of deceleration and often soaking in sea water it is advantageous to process the pellicles unsupported so that both surfaces of each sheet can be cleaned from mechanical abrasion marks prior to permanent mounting on glass for microscopy. An isothermal method for processing 1500 micron thick method unsupported pellicles and restoring them to size has been described (YAGODA, 1955, 1957, 1959).

With longer exposures to trapped and solar flare protons it has proven advantageous to employ thinner sheets of emulsion to facilitate light transmission. A study of a simplified isothermal processing procedure shows that 600 micron thick pellicles can be developed unsupported, rapidly, uniformly and essentially distortion free. The fixed gelatin sheets can be restorted routinely to their original dimensions within $\pm$ 0.5 per cent and the inner areas exhibit a distortion coefficient of less than 2 Covans. This essential freedom from track distortion is not increased in the final mounting operation, as measurements on the same tracks before and after mounting of the gelatin layer, indicates the same value of the distortion vector.

The 600 micron pellicles can be fixed in about 24 hours at 5° C. The rapid fixing of the unsupported sheets is advantageous in making trial developments as the track density can be gauged as soon as the pellicle clears. If the block has been damaged by sea water penetration, the component sheets become glued together and the standard pre-mounting techniques become inapplicable. In the new method, however, the wet block can be immersed in 5° C distilled water and as the gelatin swells the sheets can usually be pried apart with comparatively little damage. The cold water should be changed several times to help wash out the sea salts.

Because of the large gambit of exposures it is necessary to vary the developer composition to achieve a satisfactory level of light transmission. The composition of the sodium sulfite-bisulfite buffer system, which varies the pH of the developer, is described in Table IV. Formula A applicable to all low altitude probes and satellite exposures

TABLE IV

COMPOSITION OF DEVELOPER SOLUTION

Solution	*A*	*B*	*C*	*D*	*E*
Amidol, grams/liter	1.0	1.0	1.0	1.0	0.5
Sodium sulfite, Na_2SO_3	5.0	4.5	4.0	3.0	2.5
Sodium bisulfite, $NaHSO_3$	None	0.5	1.0	2.0	2.5
Potassium bromide, K Br	None	0.5	0.5	1.0	2.0
Water pre-soak, hours	1.0	1.0	1.0	1.0	2.0
Pre-soak temperature	5° C	5° C	5°	5°–1° C	5°–1° C
Developer temperature	5° C	5° C	5° C	1°–5° C	1°–5° C
Time at 1° C, hours	None	None	None	1.0	1.0
Time at 5° C, hours	6 to 16*	5	5	5.0	2.0
pH of developer	7.40	7.15	6.9	6.4	6.5

* The time in this developer can be varied to augment the grain density of minimum ionization if the track density permits. The 6 hour period is employed on low apogee satellites of one day orbiting time. Development can be extended for 16 hours on balloon exposures of 14 hours duration.

of less than 17 orbits, provided the apogee is less than 320 km, yields a grain density of 30 grains per 100 microns along the tracks of relativistic singly charged particles. With increasing orbiting time formulae B and C are employed. The weaker development reduces the grain density of the track particularly in the region where the particle is moving at high velocities. This increases the transparency without altering the count of the number of slow densely ionizing particles. Formula C has proven particularly useful on emulsions exposed for four days in polar orbits in the apogee range of 400 to 550 km. Proton tracks can be followed for about 15 mm before they become lost in the dense track background. The tracks of slow heavy primary nuclei remain of essentially the same opacity as when fully developed by formula A. Solution D proved effective in studying emulsions from Discoverer No. 18 which spent 3.14 days in orbit and reached an apogee of 704 km, well within the lower Van Allen belt.

The emulsions on board Discoverer No. 17 which was flown during a 3+ solar flare could be developed with the aid of formula E to a point where slow heavy primary tracks could be discerned above the intense single grain background produced by the solar protons (YAGODA, 1961). Here, the development procedure was greatly abetted by the photographic solarization induced by the 50 to 80 rad dosage received by the emulsion block.

Typical fields of view resulting from variation of development pH are shown in Figures 21 and 22. The conditions of exposure are too varied to describe a routine

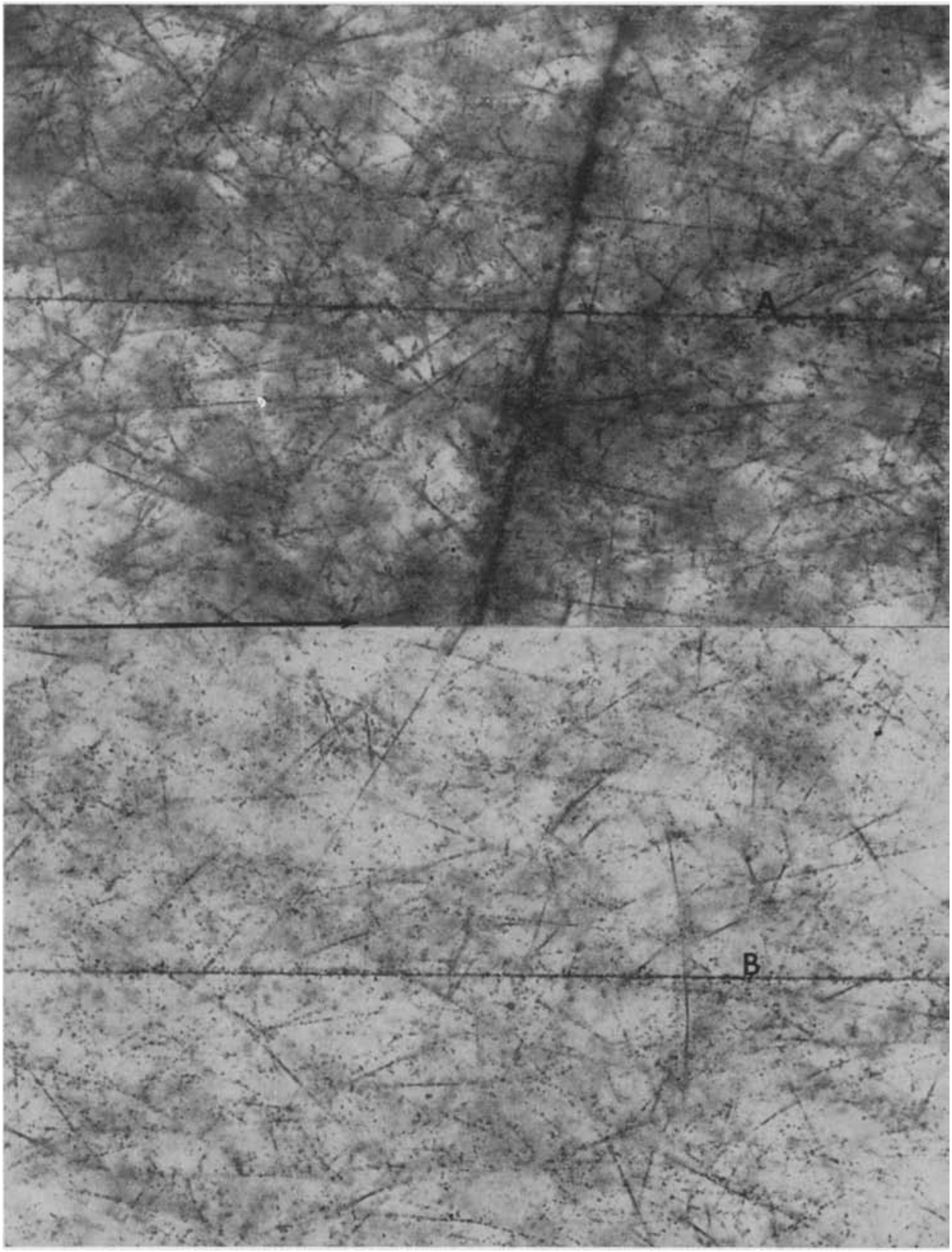

Fig. 21. Photomicrographs showing effect of developer composition and pH on track structures. Tracks A and B were produced by the same particle in the Discoverer 18 block. The preparation containing segment (A) was developed by formula A at pH 7.4, and the ligher preparation resulted from the use of formula D at pH 6.4.

processing procedure. It is good practice to make a trial run on a small portion of the block with formulae A, B and C and then decide which is best for the studies contemplated, before proceeding with the processing of the main stack. A typical schedule for the development of a block of 20 Ilford G5 pellicles measuring 10×15 cm and 600 microns thick follows:

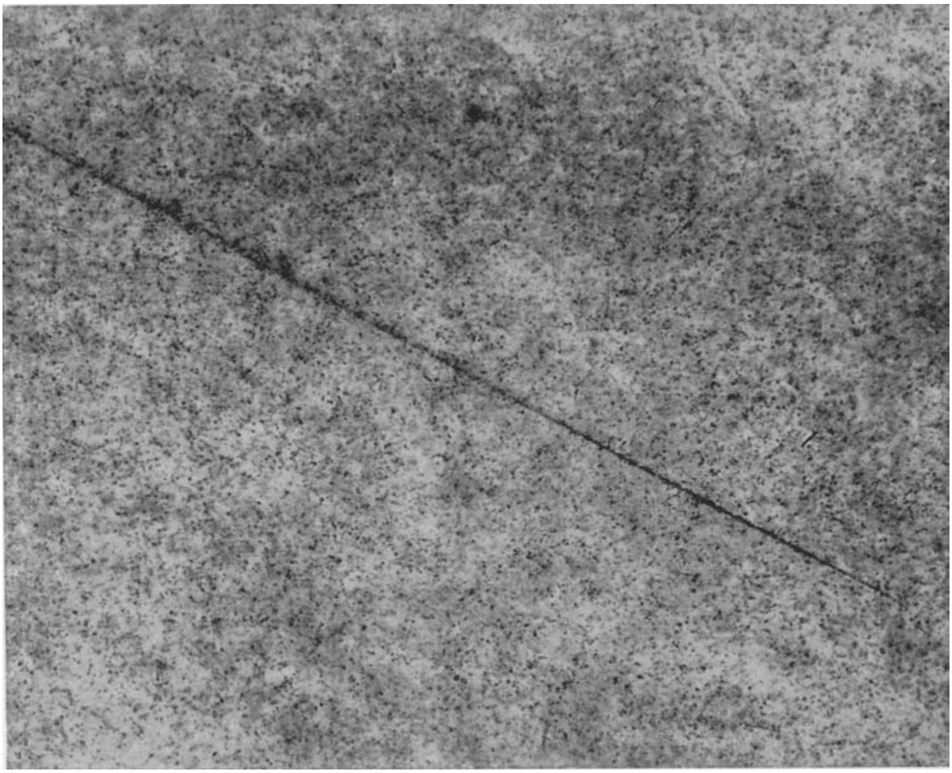

Fig. 22. Track of heavy primary nucleus developed by formula E in the solarized emulsions recovered from Discoverer 17 which was exposed to the 3+ flare of 12 November 1960. The background of 2.5×10^{10} grains per cc resulted from grains of silver bromide which received multiple hits by solar protons.

(1) Open block on arrival and inspect for moisture penetration, orientation of fiducial points (Figure 3) and identification marks. If the sheets are dry and separable, delay the processing until the following morning. If wetted by sea water initiate step (2) as soon as possible as prolonged action of the sea salts augments the fog. Meanwhile, clean 7 polyethylene or enamel trays measuring $25 \times 40 \times 5$ cm deep. Fill each with one liter of recently distilled water, lower 1 mm thick filter paper mat into the water and place trays in a refrigerator at 5° C overnight. The absorbent mats aid in bringing solution to the bottom face of the pellicle and also prevent adherence of the wet emulsion to the tray.

(2) Immerse emulsions into the trays avoiding inclusion of air bubbles. After about 30 min. of soaking, remove the sheets one at a time and gently swab the surfaces with moist cotton. This operation removes surface dirt and reduces superficial abrasion marks. The cleaned pellicles can be piled for short periods in one tray filled with cold water or appropriate solution (rinse operation).

(3) The developer solution (about 7 to 8 liters) is prepared about one hour prior to stage (1) using prechilled water. The cold trays are filled with one liter of 5° C filtered developer solution and the preswelled pellicles are maintained in it for the period described in Table IV, inverting faces every 30 min., but with no additional agitation. When the track population is low and a high minimum grain count is desired the developing period can be extended to 16 hours (overnight).

(4) Stop development by placing pellicles in 0.5 per cent acetic acid for one hour.

(5) Rinse off acid film in water and replace in trays containing about 1.3 liters of hypo at 5° C of the following composition:

Sodium thiosulfate, crystals	2270 g. (5 lbs)
Sodium sulfite	22 g.
Dilute with water too	7.5 L

The 3 per cent addition of sodium sulfite serves to increase the pH of the fixer and thus avoids resolution of developed silver image from the surface layers. During fixation the preparations tend to float, hence both surfaces should be covered with filter paper mats throughout stages (5) to (9).

(6) When the pellicles are clear (about 24 hours) rinse the sheets in 10 per cent ammonium sulfate at 5° C. Clean trays from hypo, refill with 1.3 liters of 10 per cent ammonium sulfate and allow pellicles to soak for three hours. Wash out residual hypo by rinsing in 5 per cent ammonium sulfate and soaking in trays of the 5 per cent solution overnight.

(7) Rinse in fresh 5 per cent ammonium sulfate. Transfer to trays containing 1.3 L of the following solution and maintain for 5 hours:

Thiourea	10 g.
Ammonium acetate	30 g.
Citric acid	10 g.
Dilute with water too	1 L

(8) Transfer to bath of following composition and maintain at 5° C overnight:

Thiourea	5 g.
Ammonium acetate	15 g.
Citric acid	5 g.
Ethyl alcohol	300 cc
Dilute with water too	1 L

Steps (7) and (8) serve to wash out the bulk of the ammonium sulfate, provide additional clearing action by the thiourea and reduces the pH of the gelatin to about 5, thereby inhibiting swelling. At the end of stage (8) the sheets will have shrunk appreciably, but will still be larger than the original emulsions.

(9) The wet pellicles are dehydrated by soaking in a succession of graded alcohols as follows:

EtOH	*Glycerine*	*Time*	*Temp*
40%	None	1/2 hr. rinse	5°
50%	None	2 hr. soak	5°
60%	None	1/2 hr. rinse	5°
80%	None	2 hr. soak	5°
95%	5%	Overnight	25°

(10) The surface of the dehydrated sheets (which are opaque at this stage) are cleaned gently by swabbing with cotton moistened with absolute alcohol while supported on a filter paper mat.

(11) The pellicles are supported on edge and dried in a room at high humidity, R. H. ~ 60 per cent. After several hours the gelatin will clear and when the surface ceases to be tacky the drying is completed overnight between smooth surfaced cardboards maintained under slight pressure.

(12) The completely dry pellicles are given their final cleaning prior to mounting by swabbing the surfaces with a solution composed of equal volumes of ethyl alcohol and xylene. Inspect the surface for superficially embedded linters. These can be removed by pressing down a strip of adhesive tape and then stripping it off which transfers the linters into the rubberized base.

(13) The air dried gelatin sheets are about 10 per cent smaller than the initial gelatin. They are restored to original size by soaking in a 25 per cent solution of ethyl alcohol containing a few drops of a wetting agent and 5 per cent glycerine as plasticizer. This causes swelling and after 10 to 15 min., depending on temperature and the hardness of the gelatin the sheet will approach its exposure size. The distance between fiducial marks is measured periodically and when they are identical with the imparted ones, the sheet is drained and lowered onto a sheet of subbed-glass. Air bubbles are squeezed out by brushing the surface with filter paper moistened with the swelling solution. Also, all excess fluid is drained off with the aid of the absorbent paper. As an additional precaution against curling of the edges during the final drying it is good practice to brush a film of 3 per cent gelatin solution cooled to about 25° C along the periphery. The plates are dried horizontally at a RH of about 60 per cent.

(14) As an aid to microscopy with dry objectives the mounting can be coated with a thin film of plastic. This can be effected by dipping the clean plate in a lacquer composed of one part of Duco cement and two volumes of acetone. Drain off excess fluid, support glass plate horizontally on three thumbtacks of equal height and cover with an evaporating dish whose inner walls are moistened with acetone. The film dries in about one hour and the preparation can then be examined with dry objectives. Oil immersion objectives can be employed after the lacquer film has hardened for one day. The coating operation should be executed in a relatively dust free room under conditions of moderate humidity to avoid condensation of moisture within the plastic film.

6. Studies of Star Production

The high energy particles of the cosmic radiation interact with the target nuclei of the emulsion detector producing nuclear evaporations. These events are constituted of secondary disintegration products, protons, neutrons, alpha particles and heavier spallation fragments, which leave the site of the disintegration radially and isotropically distributed. The charged secondaries produce ionization and the events are readily discerned in the emulsion as star-like structures. When the incident primary is moving at relativistic velocity meson production may precede the act of evaporation and the star will then have a collimated beam of charged π-mesons symmetrically disposed about the line of flight of the primary. Since the mean free path for star production in emulsion is known, $L_c = 150$ g. cm^{-2} the flux of the nucleonic component J_s can be estimated from the differential star count ΔP between the exposed and control emulsions

$$J_s = \Delta P L_c / \rho \omega \tag{14}$$

where ρ is the emulsion density 3.8 g. cm^{-3}. A study conducted with emulsions freshly prepared prior to the flight of Viking No. 9 (YAGODA, 1956) gave an average unidirectional flux of 0.12 ± 0.03 particles cm^{-2} sec^{-1} sterad^{-1} in good agreement with values of 0.131 ± 0.005 cm^{-2} sec^{-1} sterad^{-1} measured in counters flown above the atmosphere in rockets by VAN ALLEN (1953) and GANGNES *et al.* (1949). These fluxes while measured above the atmosphere are not a true measure of the incident primary flux as the star count is augmented by albedo particles created lower in the atmosphere and reflected upwards into the detector. The results are also rendered high by stars produced in the rocket frame which contribute a local flux of secondary star producing radiation. Recently, WADDINGTON (1960) has shown that these difficulties can be eliminated on balloon flights by tallying select stars in which the direction of the primary is determinate. WADDINGTON's estimate of 0.061 ± 0.003 protons cm^{-2} sec $^{-2}$ sterad^{-1} at $\lambda = 41°$ N indicates that at rocket elevations the flux is augmented about 50 per cent by albedo and secondary radiation.

The star count is a powerful tool for estimating the fluxes of complex radiations encountered by high altitude probes, as detailed studies of the star structures provide information on the energy of the particles producing them. The tracks associated with a star can be classified semi-quantitatively as black N_b, gray N_g and shower particles N_s. The first two components, originating largely from disintegration products of the target nucleus, are conveniently grouped together as $N_h = N_b + N_g$ and constitute tracks whose ionization is $>$ 1.4 plateau. The shower particles are defined by tracks whose grain density corresponds to $\leqq$ 1.4 plateau ionization for the particular emulsion. Stars are thus categorized by the N_h and N_s values and when the identity of the charged primary is determinate by its charge, as p-stars, α-stars and Z-stars.

When emulsions are exposed to beams of accelerated protons of known energy the relative frequency of stars with $N_h \geqq 3$ plotted against N_h yield roughly exponential functions (Figure 23), whose slopes are strongly dependent on the proton energy from 130 to 6200 Mev. At higher incident energies the change in slope is small, and as shown by EVANS *et al.* (1961) a saturation effect takes place between $E = 27$ Gev and $E \geqq 1000$ Gev. These regularities have been studies by BOZOKI and GOMBOSI (1960), LORY *et al.* (1958) have demonstrated that the N_h distribution observed in emulsions exposed to cosmic radiation can be explained by superposition of the energy dependent loci in terms of the cosmic ray energy spectrum.

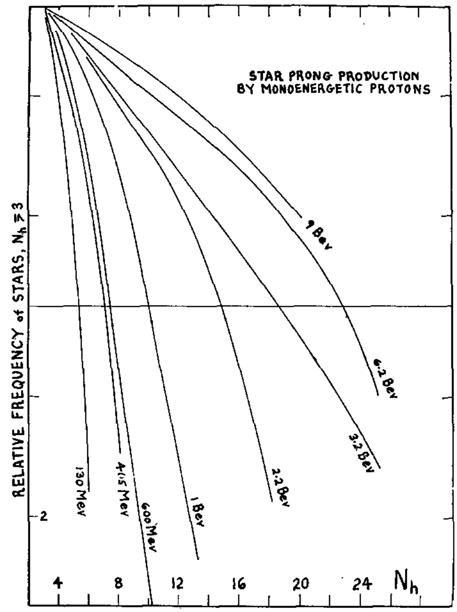

Fig. 23. Star prong spectra produced in nuclear emulsions bombarded by monoenergetic proton beams. Spectra compiled from data of (LEES, 1953) at 130 Mev, (SPRAGUE, 1954) at 405 Mev, (LOCK, 1955) at 600 Mev, (LOCK, 1955) at 1 Gev, (LORY, 1958) at 2.2 Gev, (LANNUTTI, 1955) at 3.2 Gev, (WINZELER, 1960) at 6.2 Gev, and (BOZOKI, 1960) at 9 Gev.

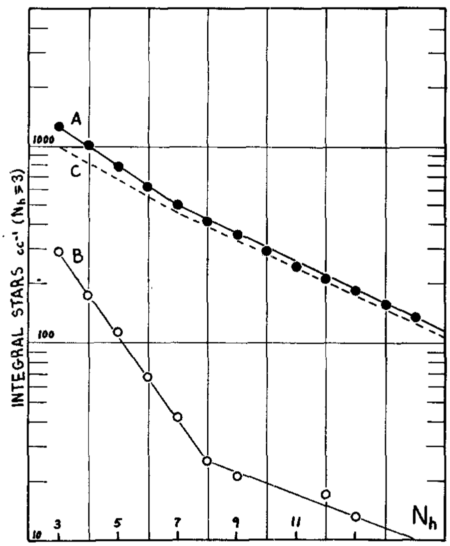

Fig. 24. Star prong spectrum (A) in emulsions exposed at 40 km at Bemidji, Minnesota during summer of 1960, and their accompanying ground controls (B). The dashed line (C) indicates the probable flight spectrum corrected for background.

Star Production Near Top of Atmosphere. When emulsions are exposed at balloon elevations (20 to 40 km) the star prong spectrum usually exhibits a break at $N_h = 6$ or 7 as shown in Figure 24 (a). The change in slope is much more pronounced in the control plates (B), the greater frequency of small stars being consistent with the lower energy of the cosmic ray particles at ground level and airplane elevations. The dashed curve C obtained by subtracting B from A thus represents the true picture of star production in the stratosphere. When the exposure is conducted at Minnesota $\lambda = 55°$ N the frequency of star production ranges between 1500 and 3300 stars cc^{-1} day^{-1} depending on altitude and time within the 11 year solar cycle. Balloon exposures at about 40° λ, similar to that of the White Sands Proving Ground, yield star frequencies of 610 to 950 cc^{-1} day^{-1}. YAGODA (1956) observed an average rate of 815 $\pm$ 104 stars cc^{-1} day^{-1} on five balloon exposures conducted furing 1952 near solar sunspot minimum. The variation of star prong spectra and frequency with geomagnetic latitude at balloon elevations is summarized in Figure 25.

Star Production in the Mesosphere. It is in general very difficult to obtain a reliable value of star production by means of vertical probes owing to the comparative short exposure period above the atmosphere. As shown in Table V, the frequency of star

TABLE V

STAR PRODUCTION ON VERTICAL ROCKET PROBES LAUNCHED AT $\lambda = 41^0$

Vehicle	*Date*	*Apogee* *km*	*Star Production** $cc^{-1}\ day^{-1}$
V-2 No. 49	29 Sept. 49	152	8060 $\pm$ 1930
Aerobee 10	5 May 52	129	6910 $\pm$ 1440
Viking 9	15 Dec. 52	218	1200 $\pm$ 284
Viking 10	7 May 54	219	1370 $\pm$ 380
Viking 11	24 May 54	255	2240 $\pm$ 570
Balloons	1952	30	815 $\pm$ 104

* Frequency computed on the basis of time spent at elevations $\geqslant \bar{h} = 2H/3$

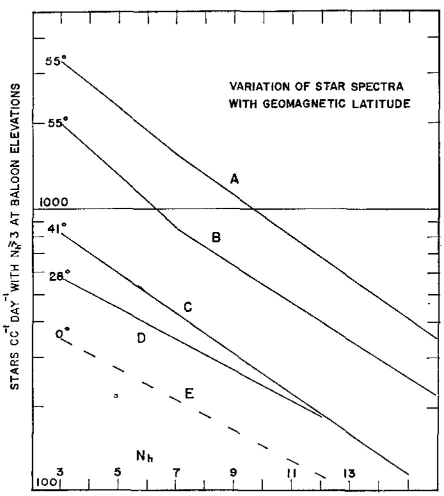

Fig. 25. Variation of star prong spectra at balloon elevations with geomagnetic latitude. Curves (A) and (B) were observed in flights at Minnesota in 1955 and 1960 and the change in absolute magnitude is due to variation of the cosmic ray intensity with time in the solar cycle. (A), (B) and (C) represent unpublished data from this laboratory. Curve (D) was constructed from the measurements of LORD (1951); and curve (E) for the equator is an extrapolation.

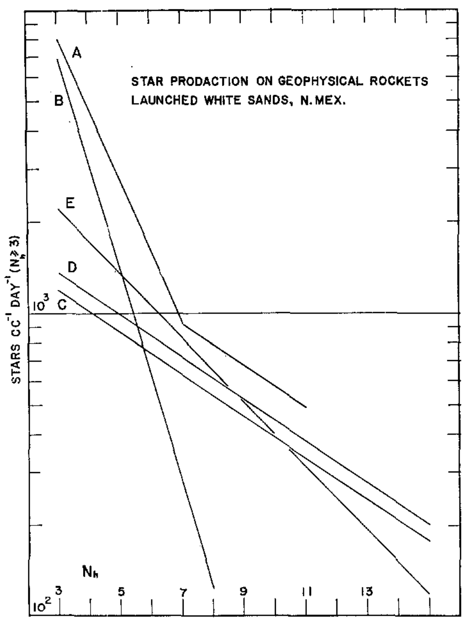

Fig. 26. Comparative star prong spectra, corrected for background, observed on several vertical rocket probes. (*A*) V-2 no. 49, (*B*) Aerobee #10, (*C*), (*D*) and (*E*) Viking rockets No. 9, 10 and 11 respectively.

production at elevations between 129 and 255 km is about 1.5 to 10 times greater than at 30 km. The lower limit is probably the most reliable estimate as the emulsions were prepared at the launching site and the ground level background was kept at a minimum of 8.75 ± 1.5 cc^{-1}. The emulsions exposed on Vikings No. 10 and 11 while prepared from Ilford gel in the laboratory, were shipped by plane to White Sands, hence these had higher background counts in the controls of 17.2 ± 1.8 and 23.7 ± 2.7 stars cc^{-1} respectively. Nevertheless, these exposures yielded values consistent with the Viking No. 9 field experiment owing to the larger volumes of emulsion that could be prepared at the home base. The V-2 and Aerobee exposures gave exceptionally high values which are difficult to reconcile in terms of altitude variation or as statistical fluctuations. These anomalous flights also exhibit markedly different star prong spectra as compared with the Viking exposures. As shown in Figure 26, the large star population recorded on the V-2 emulsions is constituted largely of small stars. These may have originated from a flux of solar protons which could reach the region sampled during a disturbance in the earth's magnetic field. The geophysical records show that this vehicle was launched 160 minutes after the appearance of a class 1 solar flare. Photon counters on board the V-2 rocket (CHUBB *et al.*, 1960) gave a count of 1.0×10^4 cm^{-2} sec^{-1} of 2–8 Å X-rays a rate about 250 to 20 times greater than measured on other rocket flights flown during quiet periods of the solar minimum sunspot cycle. This may be taken as an indication that the emulsions were exposed to the flare and the large star frequency originated from an additional flux of solar protons.

Variation of Star Production with Altitude. Within the atmosphere the frequency of star production diminishes exponentially with atmospheric depth. At elevations > 30 km the stars produced by galactic rays increase slowly as a result of increase in the effective solid angle $\bar{\omega}$ and weakening of the earth's magnetic field. The star frequency-altitude function for the White Sands geomagnetic latitude region is shown in Figure 27 (A) for altitudes up to 1000 km. This was derived by assuming that at $h \leqq 40$ km

$$I_{\text{stars}} = 935 \exp\left(-\, m_0/150\right) \text{ cc}^{-1} \text{ day}^{-1} \tag{15}$$

based on observations at 1.23 km and emulsions flown in balloons. For altitude $h > 40$ km:

$$I_{\text{stars}}(h) = \frac{935\, \bar{\omega}\,(h_i)\, j\,(h_i)}{2\pi j\,(h_{40})} \text{ cc}^{-1} \text{ day}^{-1}. \tag{16}$$

The emulsions flown on Viking rockets Nos. 9 and 10 are in good agreement with this extrapolation. This function is useful for estimating star production up to about 400 km during quiescent solar conditions. At higher elevation on additional flux of trapped protons enters the picture which greatly augments the star count extrapolated from knowledge of the galactic radiation.

Star Production in the Lower Van Allen Belt. An opportunity to study star production at elevations greater than those achieved by the Viking rockets was made possible by the recovery of a 1800 gram block of emulsions exposed on an Atlas rocket launched on 21 July 1959. This vehicle reached an apogee of 1177 km and sampled the radiations between geomagnetic latitudes 39.5° N (Cape Canaveral) and 2.2° S (Ascension Island), corresponding to an average exposure at about 21° λ. On the basis of a total period of 28 minutes, while the Atlas was above the sensible atmosphere, a frequency of 71,700 stars cc^{-1} day^{-1} with $N_h \geqq 3$ was observed (YAGODA, 1960). An analysis of the star prong spectrum showed a large predominance of small stars (98.5 per cent of $N_h < 8$) which were attributed to interactions produced by trapped protons.

These studies have been extended by the recovery of a second Atlas block and the availability of emulsions exposed by FREDEN and WHITE (1959) on a Thor-Able vehicle. The characteristics of these near equatorial flights are summarized in Table VI. On the flight of 21 July 1959 a pod of Geiger counters was ejected from the nose cone which yielded detailed information on the counting rate as a function of altitude and position along the trajectory (HOLLY, 1960). These data indicated that 90 per cent

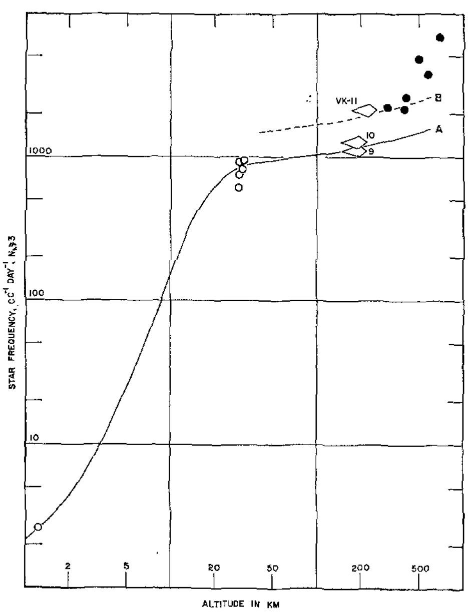

Fig. 27. Varation of star production with altitude at geomagnetic latitude 41°N. The solid line A is computed from equations (15) and (16) fitted to observations at 1.3 and 30 km. A rough estimate for star production along a polar satellite orbit is indicted by the broken line (B). The black circles represent measurements on emulsion blocks recovered from Discoverer satellites which achieved apogees between 306 and 704 km. The open circles represent balloon and mountain top measurements in the White Sands region. The diamonds represent estimates of star production on three Viking rockets.

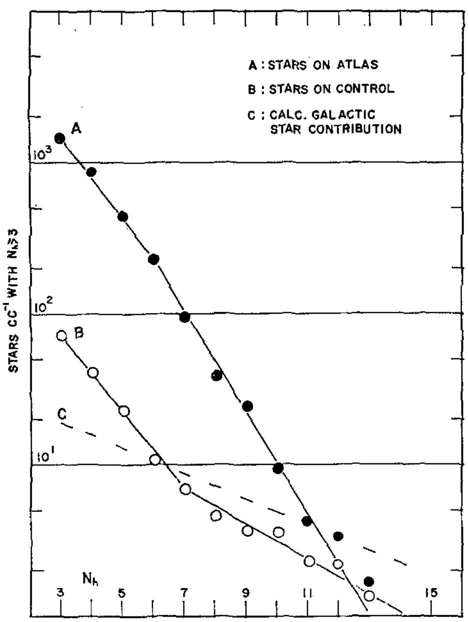

Fig. 28. Comparison of star prong spectra on emulsions flown on Atlas of 21 July 1959 (A), the controls (B) and an estimate of the galactic cosmic ray contribution (C).

of the total counts were observed during a 400-sec period when the vehicle was at altitudes between 1120 and 960 km and the geomagnetic latitude varied between 22° N and 14° N. In general, data defining the exposure period to trapped radiation is not available and the duration has been estimated on the basis of time spent at altitudes $h \geqq 2H/3$. On the basis of HOLLY's experiment the star frequencies thus calculated may be low by a factor of 2.5, but the consistent values are nevertheless useful in comparing relative altitude variations. The star production rates shown in Table VI must not be considered absolute as the limb connections to and from $h \leqq 2H/3$ could not be applied owing to the absence of experimental data in this low altitude region.

The star prong spectrum based on a study of 1653 events observed in the emulsions exposed on the 21 July 1959 Atlas are shown in Figure 28. The control plates B

TABLE VI

STAR AND PROTON ENDER FREQUENCIES ALONG NEAR EQUATORIAL TRAJECTORIES

Vehicle	*Apogee km*	*Stars* (cc^{-1} day^{-1})	*Enders* (cc^{-1} day^{-1})	*Ratio Enders to Stars*
Atlas, 21 July 1959	1177	117,000	2.1×10^6	17.9
Atlas, 13 October 1960	1185	175,000	3.4×10^6	19.4
Thor, 7 April 1959	1230	315,000	6.1×10^6	19.4

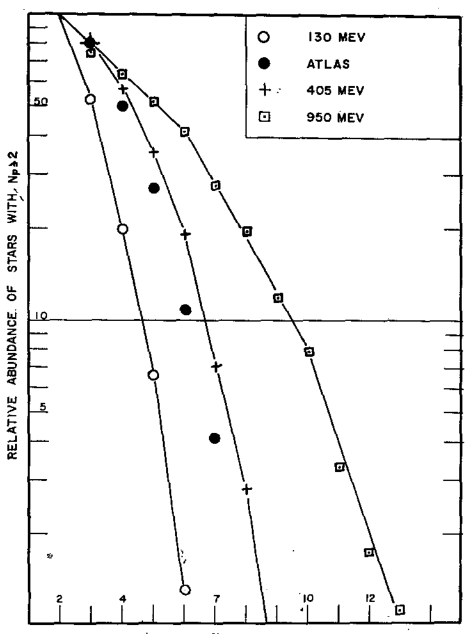

Fig. 29. Star prong spectra produced by trapped protons (black circles) compared with spectra resulting from the bombardment of emulsions with low energy monoenergetic proton beams.

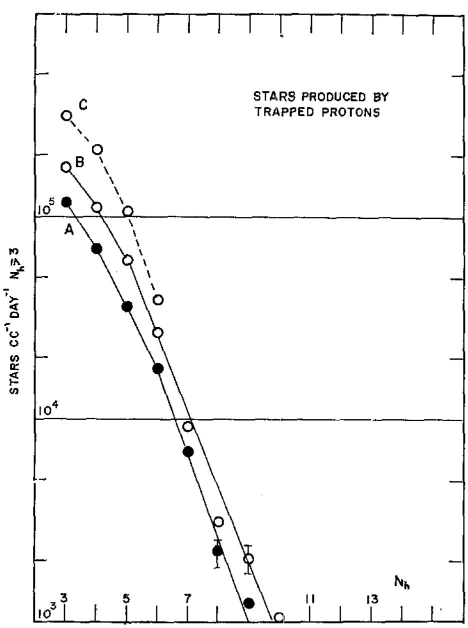

Fig. 30. Comparison of star production along near equatorial Atlas trajectories. (A) Atlas of 21 July 1959, (B) Atlas of 13 October 1960, and (C) Thor-Able of 7 April 1959.

exhibited 72 stars cc^{-1} and an estimate of the stars produced by galactic radiation averaged along the trajectory curve C of 19 cc^{-1} leaves a residual population of 1323 stars cc^{-1} which recorded during the Atlas flight. Study of Figure 28 shows that the population of large stars of $N_h \geqq 10$ is explicable in terms of the control and galactic contributions. Detailed studies show that 0.78 ± 0.10 of the stars with $N_h \leqq 8$ are associated with a gray track which can be interpreted as that of the incident trapped proton. The black and gray prong distribution N_p of this category of stars is shown in Figure 29 and is compared with star spectra resulting from the bombardment of the emulsion with monoenergetic protons. This indicates that the bulk of the small stars were produced by trapped protons with energies less than 400 Mev and having an average energy of the order of 200 to 300 Mev. In the region of 784 to 1177 km the average rate of star production by trapped protons is estimated at 117,000 cc^{-1} day^{-1} on the basis of an effective exposure of 980 sec. duration and after correction for the galactic ray contribution.

The star prong distribution observed on two Atlas flights and a Thor-Able vehicle of similar trajectory is compared in Figure 30. The spectra are similar in form, the variation in absolute rates of star production are consistent with the respective apogees of the exposures. The functions are no longer simple exponentials, and the frequency

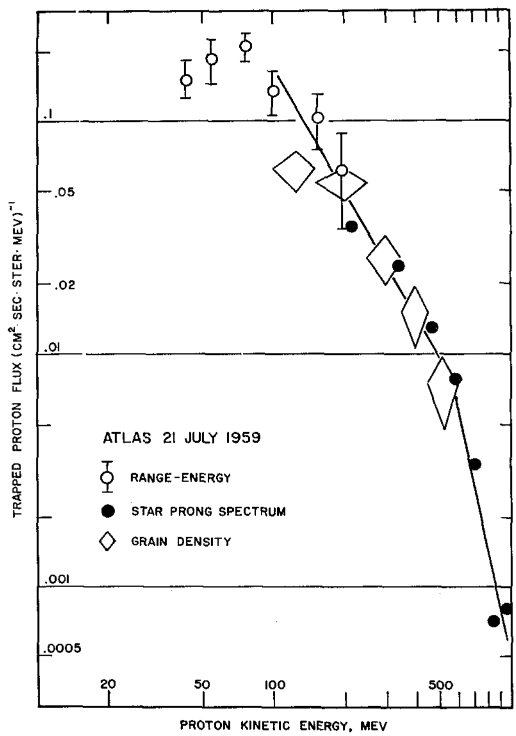

Fig. 31. Spectrum of trapped protons in the inner Van Allen belt as deduced from track ranges, grain density and star prong evaluation. The effective exposure time in the radiation belt is estimated at 400 sec.

of large stars of $N_h \geqq 6$ diminishes very rapidly. The star prong spectra can be translated into a differential energy spectrum of the trapped protons producing the interactions from the relationship

$$E(N_h - 1) = 124\,(N_h - 1) + 30 \text{ Mev} \tag{17}$$

derived by the Bristol Group (POWELL, 1959). This analysis (Figure 31) for the Atlas flown on 21 July 1959 shows that in the region of 100 to 500 Mev the flux diminishes as $1/E^{1.8}$ and at higher energies much more rapidly as $1/E^{4.8}$ As shown in Section IX this method of spectral energy determination is in good agreement with spectra derived directly from flux measurements based on range-energy relationships and the grain density of tracks.

Star Production Along Polar Satellite Orbits. Small units of nuclear emulsions have been recovered successfully after 1 to 4 days orbiting time. The characteristics of these exposures are described in Table III and the position of the blocks within the Discoverer capsule, designated E, F and J are depicted in Figure 18. The star and proton ender populations measured in the near centrally located E-position are recorded in Table VII. Owing to the integration of the cosmic and trapped radiation fluxes over all

TABLE VII

STAR AND PROTON ENDER FREQUENCIES RECORDED IN DISCOVERER EMULSION BLOCK (E)

Vehicle	*Apogee*	*Stars*	*Enders*	*Ratio Enders to Stars*
		(*cc*$^{-1}$ *day*$^{-1}$)		
D18	704	6830	144,000	21.8
D30	579	3960	77,200	19.5
D36	502	4810	73,700	15.3
D25	412	2640	23,000	8.7
D32	405	2170	25,400	11.7
D35	306	2240	18,200	8.1

latitudes and nearly all longitudes it is difficult to interpret the observations in terms of our knowledge of the galactic cosmic radiation. Discoverer 35 whose apogee was only 306 km probably represents an exposure to essentially pure cosmic radiation. On this basis, Discoverer 18 with the highest apogee in the series of 704 km shows a 3-fold increase in the star frequency. The increment originates from star production by trapped protons at points along the orbit where the inner belt has an appreciable intensity at low altitudes.

The star production-altitude profile for geomagnetic latitude 41° N is only a crude approximation to the fluxes of charged particles encountered during a polar orbit. The dashed curve B in Figure 27 is a somewhat closer approximation arrived at by integrating MEREDITH *et al.* (1955) flux measurements, made by launching rockets and rockoons at several latitudes between the equator and the magnetic poles, in terms of the time spent by a Discoverer satellite at these positions. In terms of this model, the observed star production rates up to about 450 km are reconciable with the star producing radiations of the cosmic ray beam. The deviation from curve B above 450 km is caused by additional fluxes of VAN ALLEN and solar particle radiations. Scintillation counters aboard the second and third Soviet earth satellites exposed at altitudes between 307 and 339 km show the presence of high intensity zones which cannot be explained by the latitude effect of cosmic rays (VERNOV *et al.*, 1961). The high intensity zones over Siberia and North America closely adjoins the line of maximum aurora recurrence. VERNOV attributes the anomalous zone over Brazil to penetration of the inner belt protons down to 320 km elevation. That the high star intensities exhibited by emulsions recovered from the Discoverer satellite are due to these effects is further indicated by an analysis of the star prong spectra. At low apogees the shape is similar

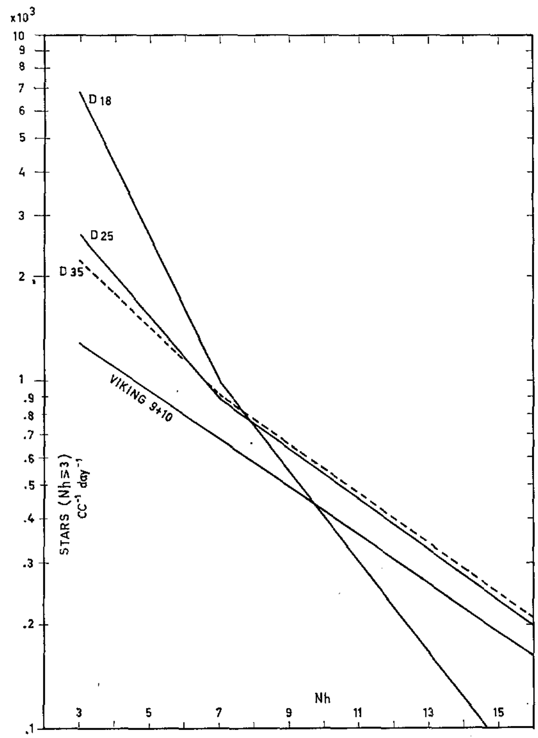

Fig. 32. Star prong spectra in emulsions recovered from Discoverer satellites. (A) Apogee 704 km, B) apogee 579 km, (C) apogee 412 km, (D) apogee 306 km. The dashed line is an average of Viking rockets No. 9 and 10 which reached apogee's of 220 km.

to that observed on Viking rocket flights. At higher apogee's the spectrum consists of two exponentials with small stars of $N_h \leqq 7$ predominating. In general, the frequency of large star production is fairly constant on the different Discoverer flights. As shown in Figure 32, Discoverer 18 is exceptional in exhibiting a rapid fall off in the large stars with $N_h > 7$. This may have originated from a large Forbush decrease which occurred while the vehicle was in orbit, as indicated by the Mt. Washington neutron monitor data Figure 33.

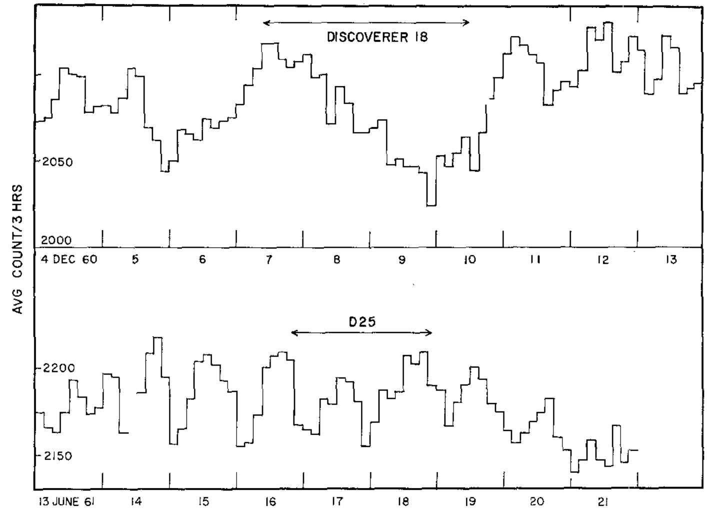

Fig. 33. Discoverer satellite exposures and cosmic ray activity as correlated by the Mt. Washington neutron monitor.

7. Proton Ender Frequencies

In 1959, WADDINGTON proposed the use of the density of particles which terminate their range in emulsion "ender tracks", as a simple parameter for studying temporal variations in the primary cosmic ray flux. In a normal exposure to galactic cosmic

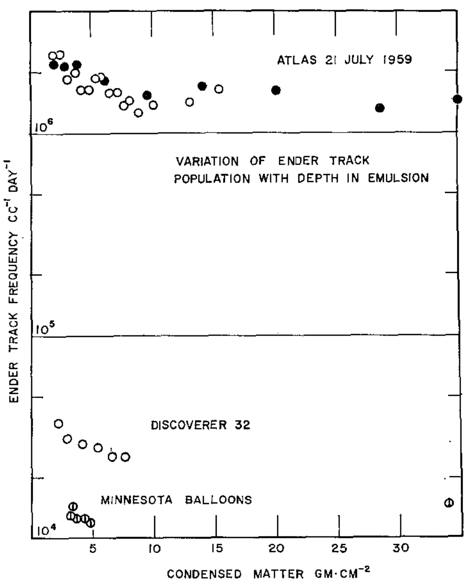

Fig. 34. Variation of proton ender frequency as a function of absorber mass, (A) in the Atlas flown 21 July 1959, (B) Discoverer No. 32 and (C) on balloon flight at 40 km.

radiation the terminating tracks largely reflect the production rate of secondary protons and alpha particles produced in nuclear disintegration processes, abetted by a small flux of low energy primaries capable of entering the emulsion detector at the particular air and geomagnetic cutoffs. It differs from a direct star count in that additional ending particles originate from proton recoils and 1- and 2-prong stars, which are not tallied in the conventional nuclear evaporation process. If the emulsion is exposed to a flux of low energy solar protons the ender density will increase, whereas the star count would remain essentially unaltered unless the solar flare also produced high energy star producing protons.

The measurement is particularly useful on high altitude probes as the ender count is a sensitive parameter for even brief exposures in the trapped radiation belt. For details of the measurement see YAGODA (1962). On balloon flights conducted at northern localities the ender frequency E is largely independent of the depth in the emulsion block and ranges between 432 and 604 ending tracks cc^{-1} $hour^{-1}$. Measurements at about 40 km elevation indicates that the ratio of enders to stars remains fairly constant, under quiescent solar conditions, and ranges between 6.1 to 7.7.

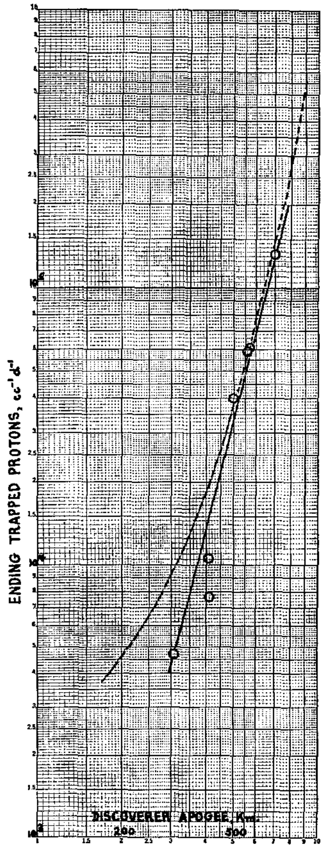

Fig. 35. Variation of ending trapped protons as a function of altitude along polar orbits.

A study of the variation of proton ender frequency with absorber mass Figure 34 in emulsion blocks flown on an Atlas trajectory and on Discoverer 32 indicates that the parameter is somewhat dependent on depth in the detector. The highest readings are obtained in the emulsion sheet facing the window. Under a total absorber of 8 g. cm^{-2}, corresponding to the range of about 80 Mev protons, the ender population is reduced about 60 percent on the Atlas and about 30 per cent on the Discoverer block. These values apply to a central area of the emulsion. When each sheet is sampled area-wise, the depth variation is less evident. The average ender frequency for several near equatorial Atlas probes and polar orbit exposures are recorded in Tables VI and VII. Data secured by WADDINGTON (1960) near the top of the atmosphere at several geomagnetic latitudes permits a rough estimate of ender production by a galactic radiation E_g along a Discoverer orbit. With apogees ranging between 306 km and 704 km E_g varies from 14,000 to 18,000 particles cc^{-1} day^{-1}. A rough estimate can thus be made of the trapped ender production $E_t = E - (E_g + E_c)$ where E_c is the ender population in the controls. Ender studies on the Discoverer emulsion blocks, Figure 35, indicate that in the region of 300 to 700 km E_t increases roughly as the fourth power of the apogee. The dashed line is an independent estimate by VAN ALLEN (1959) that the trapped proton flux doubles in intensity with each 100 km increment in

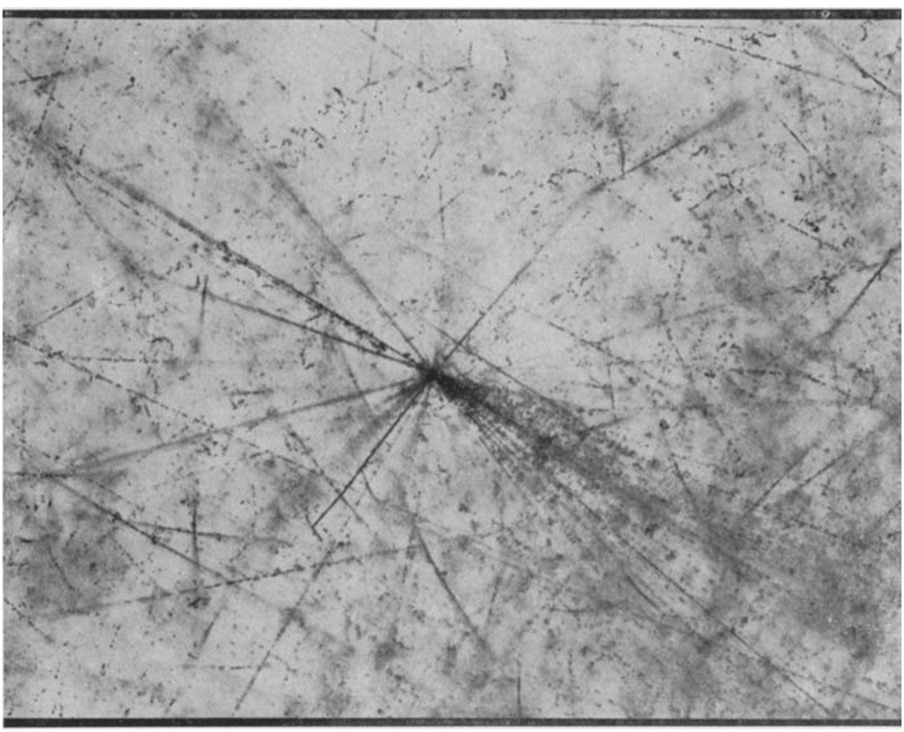

Fig. 36. Example of a central collision of a heavy primary with a silver or bromine target nucleus in which the incident particle is converted into protons and mesons.

altitude. The proton ender count is thus a useful parameter for estimating trapped radiation fluxes during quiescent periods of solar activity. Tables VI and VII show that the E/S ratio is strongly altitude dependent. At altitudes below 450 km the ratio of enders to stars is $\sim$10. Emulsions flown deeper into the trapped radiation belt give values for this ratio of about 20 for altitudes up to 1100 km.

8. The Heavy Primary Component

In 1948 FREIER *et al*, discovered the existence of a minor beam of primary particles with nuclear charges $Z \geqq 6$ incident at the top of the atmosphere. These massive multiply charged nuclei proved of considerable interest in conjunction with theories of the origin of the cosmic radiation, for details of the charge spectrum, as pointed out by BRADT and PETERS (1950) provided a measure of the time spent by the heavy primaries in the galaxy. In particular the L-nuclei composed of lithium, beryllium and boron do not occur in appreciable abundance either in the sun or stellar spectra. Their presence in the cosmic ray beam reaching the top of the atmosphere must therefore be attributed

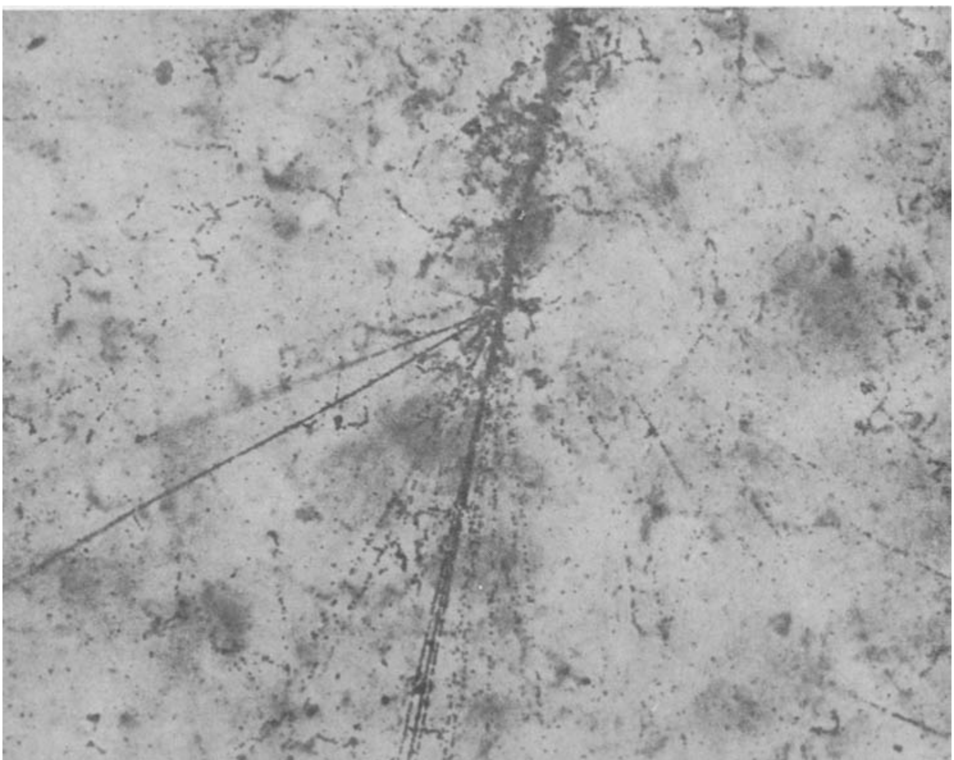

Fig. 37. Interaction of an iron nucleus in emulsion showing the production of a collimated secondary beam of L-nuclei in the forward direction and a diffuse shower of alpha particles and protons.

to collision processes of $Z \geqq 6$ (*S*-nuclei) with interstellar hydrogen and dust particles. The ratio of *L*/*S* nuclei at the top of the atmosphere proved to be very difficult to evaluate from balloon measurements within the atmosphere because of the large collision cross-sections of the *S*-nuclei. Part of the S-beam was destroyed catastrophically as indicated in Figure 36, but when the collision was peripheral, Figure 37, the initial primary fragmented into massive splinters which produced a secondary source of *L*-nuclei. Early measurements of the *L*/*S* ratio gave values ranging from 0 to 1. More recent work, where the exposure was conducted between 6 to 3 g. cm^{-2} of air, indicate a $L/S = 0.18 \pm 0.04$ (O'DELL, 1962). A critical evaluation of the balloon measurements is given in a review by WADDINGTON (1960).

Emulsions exposed in rockets are advantageous in this application as the complicated corrections for secondary *L*-nuclei production within the atmosphere are eliminated. The brevity of the exposure, however, severely limits the statistical accuracy of the flux determinations, and as explained in Section IV it is not always possible to secure a position in the rocket with a small condensed matter absorber mass. On Viking No. 10 (YAGODA, 1956) and Aerobee rockets Nos. 80 and 88 (YAGODA, 1958) the conditions were favorable for flux and charge spectra determinations. The

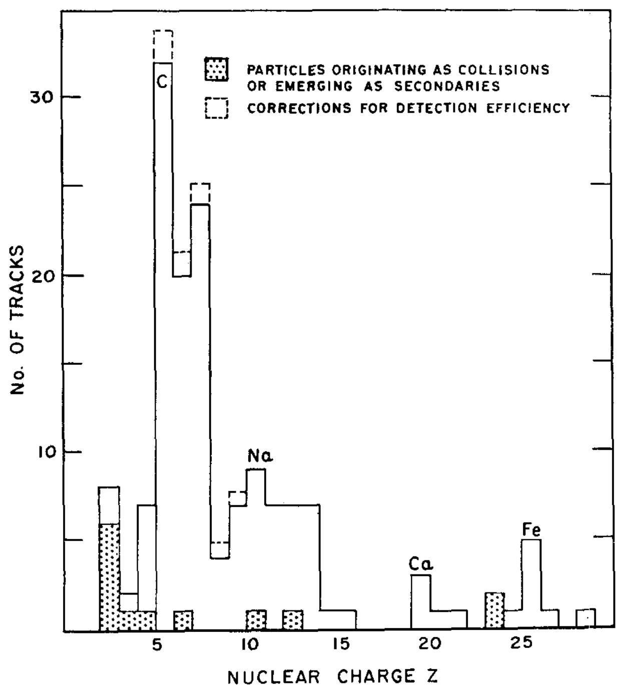

Fig. 38. Charge spectrum of *S*-nuclei as deduced from rocket probes launched at White Sands with a minimum of condensed matter surrounding the emulsions.

charge spectrum is displayed in the histogram of Figure 38, and estimates of the *L*/*S* ratio are compared in Table VIII with those obtained from more recent high altitude balloon flights.

TABLE VIII

ESTIMATES OF THE L/S RATIO AT THE TOP OF THE ATMOSPHERE DEDUCED FROM BALLOON AND ROCKET MEASUREMENTS

Investigation	*Absorber, g.cm^{-2}* air	condensed matter	L/S
Yagoda (1956)	None	2.0	0.20 $\pm$ 0.13
Waddington (1957)	20		0.26 $\pm$ 0.05
Appa Rao (1958)	7		0.058 $\pm$ 0.06
Cester (1958)	12–17		0.20 $\pm$ 0.05
Yagoda (1958)	None	$\sim$ 1.0	0.17 $\pm$ 0.06
Daniel (1962)	6.6		0.23 $\pm$ 0.09
O'Dell (1962)	2.7		0.18 $\pm$ 0.04

The comparatively long flight time of the Atlas rocket offered another opportunity to study the heavy primary charge spectrum along an equatorial trajectory. The 1800 gram block of emulsion was located at the base of the nose cone, Figure 11 (A), where the condensed matter was less than 2 g. cm^{-2} over a solid angle of 3.3 π steradians. While the average exposure from all directions averaged 5 g. cm^{-2}, a value still favorable for an L-flux determination, this did not prove feasible owing to their poor detection efficiency in the high background of trapped poton tracks. However, in a study of the interactions two events were initiated by boron nuclei, which provide a rough estimate of $L/S = 0.06 \pm 0.04$. The charge spectrum of $Z \geqq 6$ nuclei as evaluated by delta-ray density measurements (FUKUI, 1961) is displayed in Figure 39.

The heavy nuclei that escape collision ultimately lose their kinetic energy by ionization. When the particles terminate their range in emulsion the track has a characteristic needle-shape (Figure 2) which permits the ready recognition of $Z \geqq 6$ particles and the

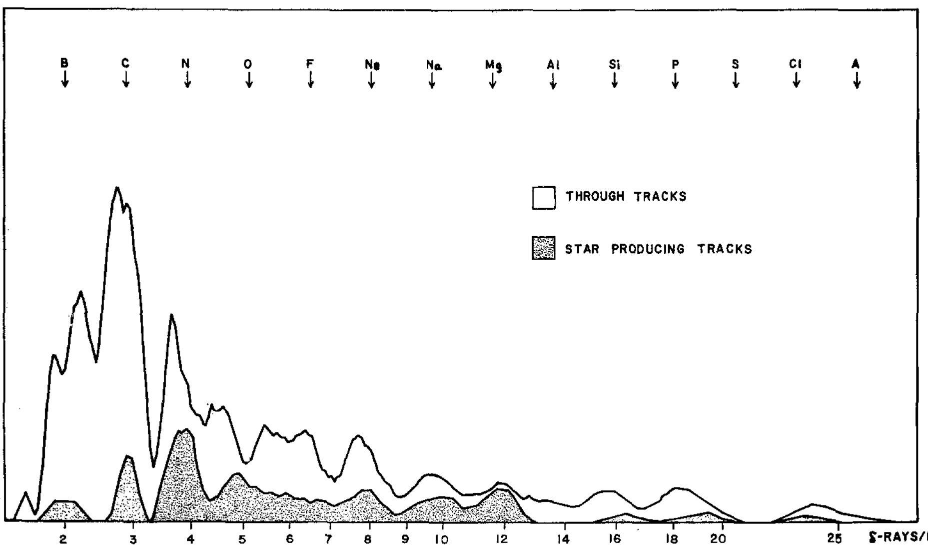

Fig. 39. Heavy primary charge spectrum along a near equatorial trajectory.

length and width of the taper region often provides an estimate of the charge. These thindown tracks offer an opportunity to study the energy spectrum of the heavy nuclei on the basis of range measurements which can be made with considerable accuracy. Satellite flights are ideal for this study since the exposure is above the airand geomagnetic-cutoffs, and the long exposure provides a statistically adequate number of events for study. The circular disks J on the Discoverer satellite (Figure 18) have an absorber mass for vertically incident particles of 1.89 g. cm^{-2}. This permits the detection of carbon nuclei with a minimum energy per nucleon of 84 Mev and an upper limit of 132 Mev per nucleon defined by the dimensions of the miniature block and the angular acceptance criteria. For a heavier particle such as silicon of $Z = 14$, these detection limits are 115 and 193 Mev per nucleon, respectively. Flux values measured on Discoverer 29 and 36 (Table IX) indicate that during periods of normal quiescient solar

TABLE IX

FLUXES OF SLOW HEAVY PRIMARY NUCLEI RECORDED ON DISCOVERER SATELLITE POLAR ORBITS

Vehicle No.	*Apogee km*	*Flux* J_M*	*(m^2. sec. sterrod)$^{-1}$* J_H**
36	502	0.17	0.13
29	563	0.14	0.09
17†	997	15.6	n.d.

* The flux covers the energy span of 84 to 132 Mev/nucleon.
** The flux covers the energy span of 115 to 193 Mev/nucleon.
† Vehicle exposed to solar flare of 12 Nov. 1960.

activity the flux in this energy region is about 2 per cent of that with $E \geqq 1$ Gev/nucleon and appears to be of constant magnitude. Emulsions recovered from Discoverer 17 which was exposed during a 3$^+$ solar flare show about a 100-fold increase in the low energy M-nuclei component (YAGODA *et al.*, 1961).

The flux and composition of the solar flare heavy nuclei has been investigated by FICHTEL and GUSS (1961) utilizing emulsion detectors launched above the atmosphere by Nike-Cajun rockets. Their flux estimates for three recent flares are summarized in Table X. An interesting feature of their charge analysis is that oxygen nuclei are more

TABLE X

FLUX OF SOLAR HEAVY NUCLEI ASSOCIATED WITH FLARES

Flare	*Time of Measurement*	*Time after flare, hours*	*Integral Flux* $J_M \geqslant 42.7$ *Mev/nuc.* *(m^2. sec. ster)$^{-1}$*
3 Sept. 1960	1498 UT	13.50	19 ± 4 (*Fichtel*, 1961)
12 Nov. 1960	1840 UT	5.30	2106 (*Biswas*, 1962)
13 Nov. 1960	1603 UT	5.70	3979 (*Biswas*, 1962)
15 Nov. 1960	1951 UT on Nov. 16	41.85	258 ± 40 (*Fichtel*, 1961)

abundant than carbon nuclei. While this agrees with estimates of the relative abundance of these elements in the sun, the reverse is the situation for the galactic heavy primaries. Within the limits of charge determination for the solarized emulsions aboard Discoverer 17, the bulk of the M-nuclei appear to be carbon. If the solar particles are accelerated to the same energies, the quantity of absorber in front of the detector will tend to modify the recorded charge spectrum. The greater absorber around the E-emulsions (2.8 g. cm^{-2}) as compared with the 0.5 g. cm^{-2} present on the Nike-Cajun flights would enhance the relative abundance of the carbon nuclei owing to their greater ranges at a fixed energy level.

The flux of solar protons during the flare of importance 3 that occurred on 3 September 1960 has been studied both by emulsions and Geiger counters (DAVIS *et al.*, 1961). The cylindrical emulsion stack was shielded by only 0.175 g. cm^{-2} of aluminum and 0.013 g. cm^{-2} of aluminized Mylar foil. This permitted the detection of protons with a minimum kinetic energy of 13 Mev. Further information on the composition of the solar flare radiation has been secured by radiochemical analysis of metals aboard Discoverer 17 exposed to the 3^+ flare of 12 November 1960. FIREMAN *et al.* (1961) observed a ratio of $H^3/H = 0.004$ in the gases isolated from the lead ballast described in Figure 18. SCHAEFFER and ZÄHRINGER (1962) found a He^3/He^4 ratio of 0.2 in the aluminum capsule exposed to the flare as compared with 0.02 for He^3/He^4 present on the surface of the quiescent sun. By studying the radioactivity induced in the silver of the emulsion block on board Discoverer 17 WASSON (1961) observed a gamma ray spectrum attributable to 8.4-day Ag^{106}. The disintegration rate indicates that the emulsion block was bombarded by a dose of 1.6×10^8 protons per cm^2.

WASSON (1962) has also isolated radioactive cobalt-57 from the stainless steel battery case (Figure 18G) flown on Discoverer 17. The concentrate which had a decay rate of 24 disintegration min^{-1} kg^{-1} of steel on 12 November 1960, corresponds to a total production of 1.3×10^7 atoms of cobalt-57 per kg., as compared with 4.8×10^8 atoms of tritium per kg of steel observed by FIREMAN *et al.*, (1961) in the same sample. WASSON's measurements clearly indicate that the tritons were not produced by an Fe^{56} (α, H^3) Co^{57} stripping reaction of the iron-56 which was present to the extent of 64 per cent abundance in the stainless steel.

9. Composition of the Inner Radiation Belt

Details of the composition and energy distribution of the charged particles in the inner radiation belt were secured by FREDEN and WHITE (1959) for those particles which penetrated the 6 g. cm^{-2} of matter surrounding the emulsions. An upper limit of one per cent was placed on the ratio of the number of electrons to protons based on a comparison of the plates flown in the Thor-Able and the controls. In the region of 75 to 700 Mev the proton energy spectrum could be represented by

$$J_p = 2100 \text{ E}^{-1.84 \pm 0.08} \text{ protons (Mev. ster. sec. cm}^2)^{-1}$$

The omnidirectional flux of protons with $E \geqq 75$ Mev was estimated at 800 ± 200

protons $cm^{-2} sec^{-1}$. In a continuation of these studies FREDEN and WHITE (May 1960) report a flux of 2 ± 1 tritons $cm^{-2} sec^{-1}$ with energies between 126 and 200 Mev. If protons were injected into the belt at the time of solar flares one would anticipate the presence of trapped helium nuclei and possibly deuterons and tritons. The observed flux of massive particles can, however, be attributed to collisions of trapped protons with air nuclei.

Emulsions have been recovered from Atlas nose cones flown on 21 July 1959 and 13 October 1960 over essentially the same trajectory sampled by the Thor-Able. The presence of thinner windows permitted an extension of the proton spectrum down to 42 Mev. In the region of 60 to 80 Mev a maximum was observed (YAGODA, July 1960) in the differential energy spectrum with a magnitude 0.62 ± 0.17 that of the flux at 76 ± 1.5 Mev. The Los Alamos group (ARMSTRONG *et al.*, February 1961) observed on the same flight a maximum at 80 Mev and a minimum at 60 Mev and attribute this fine structure in the spectrum to solar flares of class 3^+ which occurred on 10–16 July 1959, five to eleven days before the flight of the Atlas. The maximum was no longer observed on the October flight by FREDEN and WHITE (1962), however, on the same flight HECKMAN (1962) claims that it is present. The shapes of the energy distributions in the Livermore measurements are in good agreement. The ratio of the average flux measured on the October flight to that on the April is 0.6 ± 0.1. This difference originates from the 45 km higher apogee on the Thor-Able flight. The spectrum of trapped protons observed by YAGODA *et al.* (1960) on the flight of 21 July 1959 is shown in Figure 31.

The emulsions flown by NAUGLE (1962) in the NERV provide detailed information on the variation of the energy spectra with altitude and latitude. For a position in the belt comparable to that sampled by the Atlas trajectories the flux and shape of the spectra are in good agreement. At high latitudes the slope of the spectrum below 40 Mev is very steep both as compared with predictions from galactic cosmic ray neutron albedo theory and with the measurements on the Atlas flights. Two points at 1600 km elevation at λ 33.8 and 26.5° show fluxes $J(E \geqq 31)$ of 210 ± 50 and 1480 ± 270 particles $cm^{-2} sec^{-1}$. At an apogee of 1884 km and λ 30.5° the flux was 770 ± 140 particles $cm^{-2} sec^{-1}$. The energy spectrum is dependent on the magnetic shell within which the exposure was made, and considerable further effort must be expended before a detailed profile of the inner belt can be constructed.

10. Future Prospects

Lest this review appear as a canticle for a field of experimentation in which the subjects have been virtually exhausted, it is worthwhile noting some outstanding problems where the emulsion technique can contribute by its great discriminatory power. The future explorations fall into three broad categories. In the first is the search for new nuclear physics particles with large collision cross-sections that may be present in or produced by the galactic cosmic ray beam. Detailed charge and energy spectra within the newly discovered trapped radiation belts constitute a second broad category. Finally, there are the problems associated with the direct study of the cosmic ray beam as it exists in interplanetary space. While, the latter can in principle be deduced from near top of the atmosphere studies at polar localities where the charged particles are not deviated appreciably by the earth's magnetic field, direct experimental measurements at points remote from the earth might conceivably alter current notions.

At the present time some 30 singly charged fundamental particles are known varying in mass from 1 to 2580 electron masses. The mesonic particles are produced in high energy interactions and the large 30 to 50 Gev accelerators under construction would appear to be a more suitable means for detailed study than the corresponding high energy flux present in the cosmic radiation. From an astrophysical point of view, however, it would be of interest to find out whether anti-protons are present in the cosmic ray beam. A number of events (AMALDI, 1955) have been found in emulsions exposed at balloon elevations attributable to anti-proton particles. In these events the anti-particle was itself produced locally as a secondary from a high energy interaction. On a space probe with a minimum of matter surrounding the emulsions it should be possible to detect a beam of slow anti-protons, if such exists, by the characteristic large star produced in the annihilation process (BARKAS *et al.*, 1957).

The Soviet investigators (GRIGOROV *et al.*, 1961) have used this approach in a search for anti-matter over the orbit sampled by their second spaceship. The emulsions were scanned for heavy nuclei whose tracks on stopping produced an annihilation star characteristic of a multiply charged particle. None were found among 320 tracks studied. The experimental approach is good, but if the anti-matter is extragalactic in origin, and if these particles are also accelerated by the Fermi hydromagnetodynamic field mechanism one would expect to find very few low energy particles capable of stopping by ionization in the detector.

Unstable hypernuclei are known to exist with lifetimes of the order of 10^{-10} sec. It is conceivable that units of matter can be built up by substituting Λ° — particles for a fraction of the neutrons so that the resultant configuration is stable. On approaching the earth and interacting with the tenuous atmosphere less stable hyper-fragments would emerge and decay with characteristic lifetimes. If these subsequent interactions were interpreted as collision processes it would give rise to an apparent anomaly in the geometric collision mean free path. An event observed on the Viking No. 10 flight (YAGODA, 1957) in which a chain of five interactions are produced by an incident silicon nucleus may be indicative of this process. The apparent mean free path for the five interactions is about 20 times smaller than geometric and two of the interactions of $N_h = 0$ have Q-values reconcilable with the decay in flight of hyperfragments undergoing non-mesonic decay. More anomalous events of this character must be studied before their nature can be elucidated.

The charge spectrum of the $Z \geqq 20$ particles is very poorly known from balloon exposures. In part this is caused by difficulties in identification owing to photographic saturation effects and secondly by contamination of the spectrum as a result of fragments of lower charge originating from peripheral collisions of the more massive constituents with air nuclei. The latter factor can be eliminated by the exposure of near-bare emulsions in low orbiting satellites. This exposure would also help establish the presence of nuclei with charges appreciably greater than iron. It has also been postulated that the elusive Dirac monopole might produce a track in emulsion similar to that of slow heavy nuclei of $Z \geqq 10$, but differing from them in the shape of the taper (KATZ *et al.*, 1959).

With respect to studies of the trapped radiation belts it has been demonstrated that the emulsion is a useful tool for altitudes up to 1800 km. Higher altitudes would extend the exposure in fields of greater radiation intensity and make the microscopic examination of the emulsions very difficult. Thus, in the Atlas type trajectory the emulsions receive a dose of 0.28 rads using the relationship

$$W = 483\, E_t^{\,-1.646} \text{ rads hr}^{-1}$$

derived by MADEY *et al.* (1961) basis the FREDEN and WHITE energy spectrum of the trapped protons. E_t represents the energy of the protons that can penetrate the thickness of absorber surrounding the detector. On stratosphere balloon exposures 0.01 rads represents an ideal exposure from the viewpoint of microscopy and ability to resolve individual tracks produced by singly charged particles at minimum ionization. On this basis the exposure from a vertical probe reaching 1100 km apogee represents about a 30-fold burden on the emulsion detector. This can be ameliorated through the use of heavy shielding and port holes, as was done on the NERV experiment, or through the use of weaker development and scanning at higher magnifications. A probe reaching an apogee of 3000 km would receive a radiation dose of about 0.5 rads between launch and re-entry. By suitable techniques it should be still possible to evaluate the trapped proton flux, provided the launch did not coincide with an additional burst of solar protons. Because of the greater radiation level in the outer belt and the longer period spent therein, it is doubtful whether emulsions recovered from a vertical probe capable of reaching an apogee of 15,000 km would yield useful information on the composition of the outer belt.

The emulsion technique has potentialities for studying the primary galactic radiation at great distances where the earth's magnetic field can no longer perturb the direction of the particles. Techniques exist for destroying the latent image induced in the silver bromide without appreciable alteration in the basic sensitivity of the medium. Thus, in a manned flight to the moon, as an example, the dose recorded in crossing the radiation belts could be obliterated by treating the plates with oxidizing agents such as hydrogen peroxide (YAGODA, 1948) or dilute nitric acid (ACKERMANN, 1961) and restoring sensitivity when the vehicle reaches a distance of 10^5 km. Following an exposure of about 12 hours through a thin window, the emulsions could be developed in the vehicle. In principle, this eradication step could be incorporated in a non-manned spaceship which has facilities for automatic development on board. If the moon is devoid of a magnetic field, as is indicated by the Soviet lunar probes, then it is possible to study the interplanetary radiations incident on the lunar surface through the use of liquid emulsion or gel. In the initial wet condition the dispersion of silver bromide in gelatin is not sensitive to radiation. Fresh plates can thus be made in a cavern on the moon, and when dry brought to the surface for an essentially air-free cosmic ray exposure.

Acknowledgements

The launching of space probes and the recovery of their instrument sections represent complex operations whose successful culmination depends on the cooperative efforts of many people. It is not practical to mention individually all those who participated in the exposure efforts, but special thanks is given to STANLEY KRAININ of the General Electric Company for coordinating the exposures in the Atlas nose-cone and to LAWRENCE LETTERMAN and GEORGE MINALGA of the Lockheed Missiles Systems Division for the exposure of the emulsions in the Discoverer capsule. The difficult art of development was abetted by the capable assistance of ROBERT FILZ and KATSURA FUKUI. The more recent studies reported in this review were made possible by the painstaking measurements by Mrs. M. A. LANZA and Mrs. B. FILZ of the University of New Hampshire and ALBERT DAVIS and ERNEST HOLEMAN of Emmanuel College, Boston. Appreciation is expressed to Professor J. A. LOCKWOOD and M. A. SHEA, of the University of New Hampshire for the use of neutron monitor data. The star and ender data on the Thor-Able flight of 7 April 1959 was made possible by the kind cooperation of Dr. S. C. FREDEN and R. S. WHITE who provided emulsions exposed on this flight.

References

ACKERMANN, H. and H. FAISSNER, 1961, Fading in Nuclear Emulsions Induced by Acid Agents, *Nuclear Inst. Methods* **10,** 339–342.

ALEKSEEVA, K. I., L. L. GABUNIA, G. B. ZHDANOV, E. A. ZAMCHALOVA, M. I. TRETJAKOVA, and M. N. SHECHERBAKOVA, 1962, The Study of the Composition of Primary Cosmic Radiation at the Altitude of 320 km, *Journ. Phys. Soc. Japan,* **17,** Kyoto Conference Supplement A-III, 30–34.

ALPHER, R. A., 1950, Theoretical Geomagnetic Effects in Cosmic Radiation, *Journ. Geophys. Res.* **55,** 437–471.

AMALDI, E., C. CASTAGNOLI, G. CORTINI, C. FRANZINETTI and A. MANFREDINI, 1955, Unusual Event Produced by Cosmic Rays, *Nuovo Cimento* **1,** 492–500.

APPA RAO, M. V. K., S. BISWAS, R. R. DANIEL, K. A. NEELAKANTAN, and B. PETERS, 1958, Abundance of Light Nuclei in the Primary Cosmic Radiation, *Phys. Rev.* **110,** 751–765.

ARMSTRONG, A. H., F. B. HARRISON, H. H. HECKMAN, and L. ROSEN, 1961, Charged Particles in the Inner Van Allen Radiation Belt, *Journ. Geophys. Res.* **66,** 351–357.

BARKAS, W. H., R. W. BIRGE, W. W. CHUPP, A. G. EKSPONG, G. and S. GOLDHABER, H. H. HECKMAN, D. H. PERKINS, J. SANDEVEISS, E. SEGRE, F. M. SMITH, D. H. STORK, L. VAN ROSSUM, E. AMALDI, G. BARONI, C. CASTAGNOLI, C. FRANZENETTI, and A. MANFREDINI, Antiproton-nucleon Annihilation Process, *Phys. Rev.* **105,** 1037–1058.

BARKAS, W. H., 1958, The Range-Energy Relation in Emulsion, *Nuovo Cimento* **8,** 201–214.

BEISER, A., 1952, Nuclear Emulsion Technique, *Rev. Mod. Phys.* **24,** 273.

BISWAS, S., C. E. FICHTEL, and D. E. GUSS, A Study of the Hydrogen, Helium, and Heavy Nuclei in the November 12, 1960 Solar Cosmic Ray Event, *Goddard Space Flight Center Pub.* **X**-611–62–27, Greenbelt, Md.

BLAU, M. and H. Wambacher, 1937, Mitteilung über photographische Untersuchungen der schweren Teilchen in der Kosmischen Strahlung. *Sitzber. Akad. Wiss. Wien,* Abt. 2a, **146,** 623.

BOZOKI, G. and E. GOMBOSI, 1960, On the Size Distribution of Stars Observed in Nuclear Emulsions, *Acta Phys. Acad. Sci. Hungaricae* **11,** 307–316.

BRADT, H. L. and B. PETERS, 1947, Investigation of the Primary Cosmic Radiation with Nuclear Photographic Emulsions, *Phys. Rev.* **74,** 1828–1837.

BRADT, H. L. and B. PETERS, 1950, Abundance of Lithium, Beryllium, Boron and Other Light Nuclei in the Primary Cosmic Radiation and the Problem of Cosmic Ray Origin, *Phys. Rev.* **80,** 943–953.

CESTER, R., A. DEBENEDETTI, C. M. GARELLI, B. QUASSIATI, L. TALLONE, and M. VIGONE, 1958, On the Charge and Energy Spectrum of Heavy Primaries in Cosmic Radiation, *Nuovo Cimento* **7,** 371–399.

CHUBB, T. A., H. FRIEDMAN, and R. W. KREPLIN, January 1960, X-Ray Emission Accompanying Solar Flares, *Space Research* **I,** Proc. First Intern. Space Sci. Symp., Nice. North-Holland Pub. Co., Amsterdam, pp. 695–701.

DANIEL, R. R. and N. DURGAPRASAD, 1962, The Composition of Heavy Nuclei of the Primary Cosmic Radiation Above the Earth's Atmosphere, *Journ. Phys. Soc. Japan,* **17,** Kyoto conference Supplement A-III, 15–19.

DAVIS, L. R., C. E. FICHTEL, D. E. GUSS, and K. W. Ogilvie, 1962, Rocket Observations of Solar Protons on September 3, 1960, *Journ Phys. Soc. Japan,* **17**, Kyoto Conference Supplement A-II, 326–328.

DEMERS, P., *Ionographie – Les Emulsions Nucléaires,* Univ. of Montreal, 1958.

DICKINSON, M. B. and H. YAGODA, Microscopy of Thick Emulsion Pellicles, *Proc. Second Intern. Congress Corpuscular Photography,* Univ. of Montreal 1959, pp. 159–161.

ELY, J. T. A., February 1962, Atmospheric Depth and Effective Solid Angle for Radiation Penetrating the Atmosphere, *Geophysical Res. Paper* **74,** Air Force Cambridge Research Lab., Bedford, Mass.

EVANS, D. E. and R. R. HILLIER, 1961, Energy-Dependence of Fragmentation Parameters, *Nuovo Cimento* **22,** 1300–1302.

FICHTEL, C. E. and D. E. GUSS, 1961, Heavy Nuclei in Solar Cosmic Rays, *Phys. Rev. Letters* **6,** 495.

FICHTEL, C. E. and D. E. GUSS, January 1962, Heavy Nuclei in Solar Cosmic Rays, *Journ. Phys. Soc. Japan,* **17,** Kyoto Conference Supplement A-II, 321–325.

FIREMAN, E. L., J. DE FELICE, and D. TILLES, 1961, Solar Flare Tritium in a Recovered Satellite, *Phys. Rev.* **123,** 1935–36.

FREDEN, S. C. and R. S. WHITE, 1959, Protons in the Earth's Magnetic Field, *Phys. Rev. Letters* **3,** 9.

FREDEN, S. C. and R. S. WHITE, 1960, Particle Fluxes in the Inner Radiation Belt, *Journ. Geophys. Res.* **65,** 1377–1384.

FREDEN, S. C., July 1960, Nuclear Emulsion Experiments in the Inner Radiation Belt, *Abstracts Third Intern. Congress Corpuscular Photography,* Moscow, p. 53.

FREDEN, S. C. and R. S. WHITE, 1962, Trapped Proton and Cosmic Ray Albedo Neutron Fluxes, *Journ. Geophys. Res.* **67,** 25–29.

FREIER, P., E. J. LOFGREN, E. P. NEY, and F. OPPENHEIMER, 1948, The Heavy Component of Primary Cosmic Rays, *Phys. Rev.* **74,** 1818–1827.

FUKUI, K. and H. YAGODA, 1962, Heavy Primary Interactions Along An Equatorial Atlas Trajectory, *Bull. Amer. Phys. Soc.* Ser. II, **7,** 312.

GANGNES, A. V., J. F. JENKINS, and J. A. VAN ALLEN, 1949, Cosmic Ray Intensity above the Atmosphere, *Phys. Rev.* **75,** 57–69.

GRIGOROV, N. L., D. A. ZHURAVLEV, M. A. KONDRATYEVA, J. D. RAPOPORT, and I. A. SAVENKO, 1961, The Search for Anti-Matter in Cosmic Rays and in Space, *Artificial Earth Satellites,* **10,** 96–97.

HECKMAN, H. H. and A. H. ARMSTRONG, 1962, Energy Spectrum of Geomagnetically Trapped Protons, *Journ. Geophys. Res.* **67,** 1255–1262.

HOLLY, F. E. and R. G. JOHNSON, 1960, Measurement of Radiation in the Lower Van Allen Belt, *Journ. Geophys. Res.* **65,** 771–772.

KATZ, R. and D. R. PARNELL, 1959, Two Proposed Experiments for the Detection of the Dirac Monopole, *Phys. Rev.* **116,** 236–238.

LANNUTTI, J., G. GOLDHABER, and S. J. GOLDSACK, 1955, Stars Formed by Protons of 3.2 Bev from the Bevatron, *Phys. Rev.* **98,** 258.

LATTES, C. M. G., G. P. S. OCCHIALINI, and C. F. POWELL, 1947, Observations on the Tracks of Slow Mesons in Photographic Emulsions, *Nature* **160,** 453, 486.

LEES, C. F., G. C. MORRISON, H. MUIRHEAD, and W. G. V. ROSSER, 1953, The Cross Section for Star Production in Nuclear Emulsions by 130 Mev Protons, *Phil. Mag.* **44,** 304–312.

LOCK, W. O. and P. V. MARCH, 1955, Nuclear Interactions of 600 Mev Protons, *Proc. Roy. Soc.* A **230,** 222–224.

LOCK, W. O., P. V. MARCH, and MCKEAGUE, R. 1955, A Study of the Nuclear Disintegration Produced by 950 Mev Protons, *Proc. Roy. Soc.* A **231**, 368–378.

LORD, J. J. and M. S. SCHEIN, 1950, Diurnal Variation of Primary Cosmic Ray Heavy Nuclei, *Phys. Rev.* **80,** 305.

LORD, J. J., 1951, The Altitude and Latitude Variation in the Rate of Occurrence of Nuclear Disintegrations Produced in the Stratosphere by Cosmic Rays, *Phys. Rev.* **81,** 901–909.

LORY, J., C. LEFORT, and SIMONE DESPREZ-REBAUD, 1958, Interpretation de la courbe de distribution de fréquence par nombre de branches, des étoiles produites par le rayonnement cosmique dans des emulsions nucléaires, *Compt. Rend. Acad. Sci. Paris* **247,** 1185–1187.

MADEY, R., A. G. DUNEER, and T. J. KRIEGER, Sept. 1961, Proton dose Rates in Manned Space Vehicles, *Republic Aviation Corp. Pub.* **433.**

MARTIN COMPANY, October 1957, *Extra-Atmospheric Cosmic Ray Emulsion Package,* ER9793, Baltimore, Md.

MEREDITH, L. H., J. A. VAN ALLEN, and M. B. GOTTLIEB, 1955, Cosmic Ray Intensity above the Atmosphere at High Latitudes, *Phys. Rev.* **99,** 198–209.

NAUGLE, J. E. and D. A. KNIFFEN, 1961, Flux and Energy Spectra of the Protons in the Inner Van Allen Belt, *Phys. Rev. Letters* **7,** 3–6.

NAUGLE J. E. and D. A. KNIFFEN, 1962, The Flux and Energy Spectra of the Protons in the Inner Van Allen Belt, *Journ. Phys. Soc. Japan,* **17,** Kyoto Conference Supplement A-II, 118–122.

NEWELL, H. E., *High Altitude Rocket Research,* Academic Press Inc., New York, 1953.

O'DELL, F. W., M. M. SHAPIRO, and B. STILLER, 1962, Relative Abundances of the Heavy Nuclei of the Galactic Cosmic Radiation, *Journ. Phys. Soc. Japan,* **17,** Kyoto Conference Supplement A-III, 23–29.

POWELL, C. F. and G. P. S. OCCHIALINI, *Nuclear Physics in Photographs,* Oxford Univ. Press, London, 1947.

POWELL, C. F., P. H. FOWLER, and D. H. PERKINS, *The Study of Elementary Particles by the Photographic Method,* Pergamon Press, London, 1959.

PRESSLY, E. C., 1953, Air Mass between an Observer and Outer Space, *Phys. Rev.* **89,** 654–655.

ROSEN, M. W., *The Viking Rocket Story,* Harper, New York, 1955.

ROSSI, B., *High-Energy Particles,* Prentice-Hall, Inc., New York, 1952.

SCHAEFFER, O. A. and J. ZÄHRINGER, 1962, Solar Flare Helium in Satellite Materials, *Phys. Rev. Letters* **8,** 389–390.

SHAPIRO, M. M., Nuclear Emulsions, *Handbuch der Physik,* Vol. **XLV,** (ed. by S. Flügge), Springer-Verlag, Berlin, pp. 342–436.

SOBERMAN, R. K., November 1961, Micrometeorite Collection from a Recoverable Sounding Rocket, *GRD Research Note* **71,** Air Force Cambridge Research Lab., Bedford, Mass.

SPRAGUE, A. D., D. M. HASKIN, R. G. GLASSER, and M. SCHEIN, 1954, Analysis of 405 Mev Proton and 222 Mev Negative Pion Stars, *Phys. Rev.* **94,** 994–997.

VAN ALLEN, J. A., 1953, The Cosmic Ray Intensity Above the Atmosphere Near the Geomagnetic Pole, *Nuovo Cimento,* **10,** 630–647.

VAN ALLEN, J. A., C. E. MCILWAIN, and G. H. LUDWIG, 1959, Radiation Observations with Satellite 1958 Epsilon, *Journ. Geophys. Res.* **64,** 271–286.

VEPRIK, YA. M., L. V. KURNOSOVA, L. A. RAZORENOV, K. D., TOLSTOV, M. I. FRADKIN, and V. S. CHUKIN, 1961, Experience with the Development of Photoemulsion Layers aboard the Second Spaceship-Satellite, *Artificial Earth Satellites,* **10,** 34–41.

VERNOV, S. N., E. V. GORCHAKOV, YU. I. LOGACHEV, V. E. NESTEROV, N. F. PISARENKO, I. A. SAVENKO, A. E. CHUDAKOV, and P. I. SHAVRIN, 1962, Investigations of Radiation during Flights of Satellites, Space Vehicles and Rockets, *Journ. Phys. Soc. Japan* **17,** Kyoto Conference Supplement A-II, 162–187.

WADDINGTON, C. J., 1957, The Charge Distribution of Multiply Charged Nuclei in the Primary Cosmic Radiation, *Phil. Mag.* **2,** 1059–1078.

WADDINGTON, C. J., 1959, The Study of Cosmic Ray Variations with Nuclear Emulsions, *Nuovo Cimento* **14,** 1205–1216.

WADDINGTON, C. J., 1960, The Determination of the Flux of Cosmic Ray Protons with Nuclear Emulsions, *Phil. Mag.* **5,** 1105–1117.

WADDINGTON, C. J., The Composition of the Primary Cosmic Radiation, *Prog. Nuclear Physics,* Vol. VIII, Pergamon Press, Oxford, 1960, pp. 1–45.

WADDINGTON, C. J., 1960, Note on Ending Particles in Nuclear Emulsions exposed to the Primary Cosmic Radiation, *Nuovo Cimento* **18,** 820–822.

WASSON, J. T., 1961, Radioactivity produced in Discoverer No. 17 by November 12, 1960 Solar Protons, *Journ. Geophys. Res.* **66,** 2659–2663.

WASSON, J. T., April 1962, Radioactive Cobalt and Manganese in Discoverer 17 Stainless Steel, *AFCRL Studies of the November* 1960 *Solar-Terrestrial Events* (ed. by J. Aarons and S. M. Silverman), AFCRL–62–441.

WIDGOFF, M., Nuclear Emulsions, *Techniques of High Energy Physics* (ed. by D. M. Ritson), Interscience Publ., Inc., New York, 1961, pp. 115–205.

WINZELER, H., B. KLAIBER, W. KOCH, M. NIKOLIC, and M. SCHNEEBERGER, 1960, Interactions of 6.2 Gev Protons in Emulsions, *Nuovo Cimento* **17,** 8.

YAGODA, H. and N. KAPLAN, 1948, Background Eradication by Accelerated Fading of the Latent Image, *Phys. Rev.* **73,** 634–635.

YAGODA, H., *Radioactive Measurements with Nuclear Emulsions,* John Wiley and Sons, Inc., New York, 1949.

YAGODA, H., H. DE CARVALHO, and N. KAPLAN, 1950, Stars and Heavy Primaries Recorded during a V-2 Rocket Flight, *Phys. Rev.* **76,** 765-767.

YAGODA, H., 1955, Isothermal Processing of Thick Nuclear Emulsions, *Rev. Sci. Inst.,* **26,** 263–266.

YAGODA, H., 1956, Observations on Stars and Heavy Primaries Recorded in Emulsions Flown in Viking Rocket No. 9, *Canadian Journ. Physics* **34,** 122–146.

YAGODA, H., 1956, Abundance of Lithium, Beryllium and Boron Nuclei at the Top of the Atmosphere, *Bull. Am. Phys. Soc.*, Ser. II, **1,** 229.

YAGODA, H., July 1957, Une méthode isothermique améliorée pour le traitement des pellicules épaisses d'émulsions nucléaires, *Proc. First Intern. Congress Corpuscular Photography,* Strasbourg, pp. 247–254.

YAGODA, H., July 1957, Cassettes d'émulsions pour l'étude des rayons cosmiques dans les fusées a haute altitude, *Proc. First Intern. Congress Corpuscular Photography,* Strasbourg, pp. 423–432.

YAGODA, H., 1957 Anomolous Heavy Primary Cascades Recorded on Viking No. 10 Rocket Flight, *Nuovo Cimento* **6,** 559–570.

YAGODA, H., May 1957, Micro-meteorite Observations from the Flight of USAF Aerobee No. 77, *Geophysics Research Directorate,* Air Force Cambridge Res. Center, Bedford, Mass.

YAGODA, H., July 1958, Observations on Heavy Primary Cosmic Ray Nuclei above the Atmosphere, *Geophysical Research Paper* **60,** AF Cambridge Res. Center, Bedford, Mass.

YAGODA, H., 1960, Star Production by Trapped Protons in the Inner Radiation Belt, *Phys. Rev. Letters* **5,** 17–18.

YAGODA, H., 1960, The Recovery of Cosmic Ray Emulsions from Rocket and Space Probes, *Physics Today* **13,** 18–25.

YAGODA, H., April 1961, Cosmic Radiation Studies on Manhigh III Flight, *AF Missile Development Center, Technical Rep.* **60–16,** Holloman AFB, New Mexico, pp. 189–197.

YAGODA, H., 1961, Radiation Studies from Nuclear Emulsions and Metallic Components Recovered from Polar Satellite Orbits, *Proc. Second Intern. Space Science Symp.,* Florence, 849–866.

YAGODA, H., R. FILZ, and K. FUKUI, 1961, Emission of Carbon Group Heavy nuclei from a 3^+ Solar Flare, *Phys. Rev. Letters* **6,** 526–527.

YAGODA, H., February 1962, Bioastronautical Measurements of Ionizing Radiations in Space: Nuclear Emulsion Monitoring Report, *Geophysics Res. Note* **76,** Air Force Cambridge Res. Lab., Bedford, Mass.

YNGVE, V. H., 1953, The Time Variation of Cosmic Ray Heavy Nuclei, *Phys. Rev.* **92,** 428–435.

YUKAWA, H., 1935, On the Interaction of Elementary Particles, *Proc. Phys. – Math. Soc., Japan* **17,** 48.